

Formation of Jupiter and Conditions for Accretion of the Galilean Satellites

P. R. Estrada, I. Mosqueira, J. J. Lissauer, G. D'Angelo, D. P. Cruikshank

Abstract

We present an overview of the formation of Jupiter and its associated circumplanetary disk. Jupiter forms via a combination of planetesimal accretion and gravitational accumulation of gas from the surrounding solar nebula. The formation of the circumjovian gaseous disk, or subnebula, straddles the transitional stage between runaway gas accretion and Jupiter's eventual isolation from the solar disk. This isolation, which effectively signals the termination of Jupiter's accretion, takes place as Jupiter opens a deep gas gap in the solar nebula, or the solar nebula gas dissipates. The gap-opening stage is relevant to subnebula formation because the radial extent of the circumjovian disk is determined by the specific angular momentum of gas that enters Jupiter's gravitational sphere of influence. Prior to opening a well-formed, deep gap in the circumsolar disk, Jupiter accretes low specific angular momentum gas from its vicinity, resulting in the formation of a rotationally supported compact disk whose size is comparable to the radial extent of the Galilean satellites. This process may allocate similar amounts of angular momentum to the planet and the disk, leading to the formation of an *ab-initio* massive disk compared to the mass of the satellites. As Jupiter approaches its final mass and the gas gap deepens, a more extended, less massive disk forms because the gas inflow, which must come from increasingly farther away from the planet's semimajor axis, has high specific angular momentum. Thus, the size of the circumplanetary gas disk upon inflow is dependent on whether or not a gap is present. We describe the conditions for accretion of the Galilean satellites, including the timescales for their formation, and mechanisms for their survival, all within the context of key constraints for satellite formation models. The environment in which the regular satellites form is tied to the timescale for circumplanetary disk dispersal, which depends on the nature and persistence of turbulence. In the case that subnebula turbulence decays as gas inflow wanes, we present a novel mechanism for satellite survival involving gap opening by the largest satellites. On the other hand, assuming that sustained turbulence drives subnebula evolution on a short timescale compared to the satellite formation timescale, we review a model that emphasizes collisional processes to explain satellite observations. We briefly discuss the mechanisms by which solids may be delivered to the circumplanetary disk. At the tail end of Jupiter's accretion, most of the mass in solids resides in planetesimals of size > 1 km; however, planetesimals in Jupiter's feeding zone undergo a period of intense collisional grinding, placing a significant amount of mass in fragments < 1 km. Inelastic or gravitational collisions within Jupiter's gravitational sphere of influence allow for the mass contained in these planetesimal fragments to be delivered to the circumplanetary disk either through direct collisional/gravitational capture, or via ablation through the circumjovian gas disk. We expect that planetesimal delivery mechanisms likely provide the bulk of material for satellite accretion.

1. INTRODUCTION

The prograde, low inclination orbits and close spacing of the regular satellites of the four giant planets indicate that they formed within a circumplanetary disk around their parent planet. The fact that all of the giant planets of our Solar System harbor families of regular satellites suggests that satellite formation may be a natural, if not inevitable, consequence of giant planet formation. Thus to understand the origins of the Jovian satellites, we must understand the formation of Jupiter and its circumplanetary disk.

Observations provide some basic constraints on Jupiter’s origin. Jupiter must have formed prior to the dissipation of the solar nebula because H and He (the planet’s primary constituents) do not condense out at any location in the protoplanetary disk; therefore these light elements were accumulated in gaseous form. Protoplanetary disks are observed to have lost essentially all of their gases in $< 10^7$ years (*Meyer et al.*, 2007), e.g., by photoevaporation (*Shu et al.*, 1993; *Dullemond et al.*, 2007), implying that Jupiter must have completed its formation in no longer than this time. A fundamental question of giant planet formation is whether Jupiter formed by analogy to the Sun as a result of a gravitational instability that occurred in the solar nebula gas, or through accretion of a solid core that eventually became large enough to accumulate a gaseous envelope directly from the nebula. The evidence supports the latter formation scenario in which the early stage of planetary growth consists of the accumulation of planetesimals, analogous to the consensus treatment of terrestrial planets (*Lissauer and Stevenson*, 2007; cf. *Durisen et al.*, 2007). The heavy element core grows sufficiently large ($\sim 5 - 10 M_{\oplus}$, where $M_{\oplus} = 5.976 \times 10^{27}$ g is an Earth mass) that it is able to accrete gas from the surrounding nebula (*Hubickyj et al.*, 2005). The planet’s final mass is dictated by either the opening of a gas gap in the protoplanetary disk, or the eventual dissipation of the solar nebula. Jupiter’s atmosphere is enhanced in condensible material by a factor of $\sim 3 - 4$ times solar (and $\sim 3 - 8$ times overall, depending on core size). This observation suggests that the Jovian subnebula may also have been enhanced in solids with respect to solar composition mixtures.

The enhancement of solids in Jupiter’s gaseous envelope, the composition of its core, and ultimately the source material that went into making the Jovian satellite system, likely reflect the composition of planetesimals that formed within its vicinity as well as farther out in the circum-solar disk. Observed variations of the oxygen isotopic composition among meteorite parent bodies, and even differences of composition of a variety of trace elements as well as oxygen within a single meteorite (e.g., *Clayton et al.*, 1985; *Boynnton*, 1985; *Clayton*, 1993; 2003; *Scott and Krot*, 2005; *Yurimoto et al.*, 2007), indicates that the early solar nebula was not homogeneous. This inhomogeneity is further exemplified by the composition of comets, which contain grains with a wide range of volatility (*Brownlee et al.*, 2006; *Zolensky et al.*, 2006). For example, dust samples from Comet 81P/Wild 2 brought to Earth by the Stardust space mission show a great diversity of high- and moderate-temperature minerals, in addition to organic material (e.g., *Brownlee et al.*, 2006; *Sandford et al.*, 2006). The great chemical complexity and variety of the organics appear to reflect different mechanisms of synthesis at a range of times and in various locales, although the process of capture of the Stardust samples may have induced further chemical alteration (*Cody et al.*, 2007).

The implication from these observations is that there was a significant amount of radial mixing within the early solar nebula leading to the transport of high temperature minerals from the innermost regions of the solar nebula to beyond the orbit of Neptune. These high temperature minerals could have been transported from in the inner Solar System to the outer edge either through ballistic transport above the midplane (*Shu et al.*, 2001), or turbulent transport in the midplane (*Scott and Krot*, 2005; *Cuzzi et al.*, 2005; *Cuzzi and Weidenschilling*, 2006; *Natta et al.*, 2007; *Ciesla*, 2007). In the latter “X-wind” model proposed by *Shu et al.* (2001), Shu and colleagues predicted that there would be transport of CAIs (calcium- aluminum-rich inclusions) from near the Sun to the outer edge of the Solar System where Comet Wild 2 formed. Once transported, these minerals may have been incorporated into the first generation of planetesimals that went into making Jupiter and the outer planets. The presence of super-solar abundances of more volatile species such as argon (which requires very low temperatures to condense) in Jupiter’s atmosphere implies that, in addition to outward transport of high temperature material, there was also inward transport of *highly* volatile material within solid bodies (e.g., *Cuzzi and Zahnle*, 2004; *Ciesla and Cuzzi*, 2006); see Sec. 2.4. Similar evolution might also have characterized circumplanetary nebulae at some stage in their

evolution.

The formation of giant planet satellite systems has been treated as a poorly understood extension of giant planet formation (see, however, early work by *Coradini et al.*, 1981; 1982). Thanks in great part to the success of the Voyager and Galileo missions, the Jovian satellite system has been studied extensively over the last three decades; the emphasis has been on the Galilean satellites Io, Europa, Ganymede, and Callisto, a magnificent quartet of unique planetary bodies in their own right. One of the more profound realizations about the Jovian satellite system is that its cosmochemical and dynamical properties may provide important clues about the late and/or post-accretional stages of Jupiter’s formation (*Pollack and Reynolds*, 1974; *Mosqueira and Estrada*, 2003a,b; *Estrada and Mosqueira*, 2006).

The abundances and the chemical form of constituents observed in the Jovian satellite system are a diagnostic of their source material (i.e., whether or not the material condensed in the solar nebula or was it re-processed/condensed in the subnebula). However, interpretation of their cosmochemical properties is complicated because objects the size of the Galilean satellites could have been altered through extensive resurfacing due to differentiation, energetic impacts, and other forms of post-accretional processing that may have occurred after their formation. Callisto and Ganymede have mean densities of 1.83 and 1.94 g cm⁻³, respectively; each consists of $\sim 60\%$ rock, and $\sim 40\%$ water-ice by mass (*Sohl et al.*, 2002). In contrast, solar composition contains $\sim 60\%$ water-ice, $\sim 40\%$ rock by mass. This may indicate that Callisto and Ganymede lost some water during their accretion. However, the amount of water in Europa (3.01 g cm⁻³) is only $\sim 5\%$ by mass. If the initial composition was like that of its outer neighbors, its current state requires additional mechanisms to explain its water loss. On the other hand, Io has a mean density (3.53 g cm⁻³) consistent with rock. Thus, a key feature of the Galilean satellite system is the abrupt decrease in ice fraction as one approaches Jupiter.

Yet, despite this remarkable radial trend in water-ice fraction, the largest of the tiny moons orbiting interior to Io, Amalthea, has a density so low that even models for its composition that include unreasonably high choices for its porosity require that water-ice be a major constituent (*Anderson et al.*, 2005). The lack of mid-sized moons, which could provide additional clues to the relative abundances of rocky and icy material, complicates our attempts to understand the cosmochemical history of the Jovian system. Contrast this with the Saturnian system, where the average density of the regular, icy satellites (~ 1.3 g cm⁻³) allows us to infer a non-solar composition or the presence of a significant amount of low-density hydrocarbons (e.g., *Cruikshank et al.*, 2007a,b), which are presumed to have density ~ 1.1 g cm⁻³. Still, satellites in the Jovian system are found to contain evidence of hydrocarbons through their spectral signatures in the low-albedo surface materials (e.g., *Hibbitts et al.*, 2000, 2003; *Clark et al.*, 2005), and possibly CN-bearing materials (*Cruikshank et al.*, 2005). Whether these materials are intrinsic or extrinsic (e.g., a coating from impactors) in origin is not known.

Although one can think of Jupiter and its satellites as a “mini Solar System”, there are several fundamental differences between accretion in a circumplanetary disk and the solar nebula. In the circumplanetary disk, thermodynamical properties, length scales, and dynamical times are much different than their circumsolar analog. Most of these differences can be attributed to the fact that giant planet satellite systems are quite compact. For instance, the giant planets dominate our Solar System in angular momentum; however, the analogy does not extend to the Galilean system where the majority of the system angular momentum resides in Jupiter’s spin. Moreover, dynamical times, which can influence a number of aspects of the accretion process, are orders of magnitude faster in circumplanetary disks than in the circumsolar disk (accretion of planets in the habitable zones of M dwarf stars are an intermediate case, *Lissauer*, 2007). As an example, Europa’s orbital

period is $\sim 10^{-3}$ times that of Jupiter. This may have consequences for the coagulation of dust to satellitesimals (the circumplanetary equivalent of planetesimals) in the circumjovian disk.

Over the last decade, there have been a number of global models of the Jovian satellite system designed to fit the observational constraints provided by the Voyager and Galileo missions (*Mosqueira and Estrada*, 2000, 2003a,b; *Estrada*, 2002; *Canup and Ward*, 2002; *Mousis and Gautier*, 2004; *Alibert et al.*, 2005a; *Estrada and Mosqueira*, 2006). Key constraints for models of the Galilean satellite system are as follows:

1. The angular momentum contained within the Galilean satellites serves as a firm constraint on the system. Aside from explaining its overall value, one must also explain why there is so much angular momentum (and mass) in Callisto (nearly as much as Ganymede), yet no regular satellites outside its orbit.
2. The increase in ice fraction with distance from the planet for the Galilean satellites (a.k.a., compositional gradient) is often attributed to a temperature gradient imposed by the proto-Jupiter or Jovian subnebula. However, this remains a somewhat weak constraint because it is debatable whether the compositions of Io and Europa, specifically, are primordial or altered by mechanisms (e.g., tidal heating, hypervelocity impacts) that would preferentially strip away volatiles. Moreover, Amalthea’s low density strongly suggests that water-ice is a major constituent of this inner, small satellite.
3. The moment of inertia of Callisto suggests a partially differentiated interior provided hydrostatic equilibrium is assumed (*Anderson et al.*, 1998; 2001). This implies that Callisto must be put together slowly ($\gtrsim 10^5$ years, *Stevenson et al.*, 1986). However, it may be possible that a nonhydrostatic component in Callisto’s core could be large enough to mask complete differentiation (*McKinnon.*, 1997).
4. The nearly constant mass ratio of the largest satellites of Jupiter and Saturn (and possibly Uranus) to their parent planet, $\mu \sim 10^{-4}$, suggests that there may be a truncation mechanism that limits satellite mass (*Mosqueira and Estrada*, 2003b).

This chapter is organized as follows. In Section 2, we present a detailed summary of the currently favored model for the formation of Jupiter. In Sec. 3, we discuss the formation of the circumjovian disk. In Section 4, we address the possible environments that arise for satellite formation during Jupiter’s late stage of accretion. We summarize the processes involved in the accretion of Europa and the other Galilean satellites, the methods of solids mass delivery, timescales for formation, and discuss the key constraints in more detail. In Section 5, we present a summary.

2. FORMATION OF JUPITER

Jupiter’s accretion is thought to occur in a protoplanetary disk with roughly the same elemental composition as the Sun; that is, primarily H and He with $\sim 1 - 2\%$ of heavier elements. A lower bound on the mass of this solar disk of $\sim 0.01 - 0.02 M_{\odot}$ (where $M_{\odot} = 1.989 \times 10^{33}$ g is the mass of the Sun) has been derived from taking the condensed elemental fractions of the planets of the Solar System and reconstituting them with enough volatiles to make the composition solar. This is historically referred to as the “minimum mass solar nebula” (MMSN, *Weidenschilling*, 1977b; *Hayashi*, 1981). The radial distribution of solids is found by smearing the augmented mass of the planet over a region halfway to each neighboring planet. This approach yields a trend in surface density (by design, both in solids and gas) with semimajor axis, r , of $\Sigma \propto r^{-3/2}$ between Venus

and Neptune (*Weidenschilling*, 1977b). In this picture, it is implicitly assumed that the planets form near their present locations. This means that planetary formation is characterized by “local growth” – that is, the planets accreted from the reservoir of gas and solids that condensed within their vicinity. Given the super-solar heavy volatile element abundances in Jupiter’s atmosphere, the distribution of solids in the solar nebula is often enhanced (by a factor of several above the MMSN) at the location of Jupiter where a “jump” in solids surface density is attributed to the water-ice condensation/evaporation front (often referred to as the “snow line”). However, the Jovian atmosphere contains enhancements above solar in noble gases such as argon (which condenses at very low temperature, see Sec. 2.4), so that even with a modification in the surface density, a local growth model likely does not do a good enough job of explaining the composition of the giant planets because it would require local temperatures much lower than even the most optimistic of disk thermal structure models.

The radial temperature of the photosphere of the solar nebula is commonly taken to be that derived from assuming that the disk is optically thin (to its own emission), and dust grains are in radiative balance with the solar luminosity ($T \propto r^{-1/2}$, *Pollack et al.*, 1977; *Hayashi*, 1981). This temperature dependence is one that might be expected from the accumulation of most of the mass in larger bodies, which is implicitly assumed during the planetary formation epoch. However, efforts to match the spectral energy distributions of circumstellar disks around T Tauri stars have spawned a number of alternative disk models that lead to different thermal disk structures (e.g., *Kenyon and Hartmann*, 1987; *Chiang and Goldreich*, 1997; *Garaud and Lin*, 2007). These uncertainties in the most fundamental of disk properties underlie some of the reasons why the formation of giant planets remains one of the more scrutinized problems in planetary cosmogony today (see, e.g., recent reviews by *Wuchterl et al.*, 2000; *Hubbard et al.*, 2002; *Lissauer and Stevenson*, 2007).

Of the two formation models for giant planets that have received the most attention, the preponderance of evidence supports the formation of Jupiter via *core nucleated accretion*, which relies on a combination of planetesimal accretion and gravitational accumulation of gas. The alternative, the so-called *gas instability model*, would have Jupiter forming directly from the contraction of gaseous clump produced through a gravitational instability in the protoplanetary disk. In this model, formation of Jupiter is somewhat akin to star formation. Although numerical calculations have produced $\sim 1 M_J$ (where $M_J = 1.898 \times 10^{30}$ g is a Jupiter mass) clumps in sufficiently unstable disks (e.g., *Boss*, 2000; *Mayer et al.*, 2002), the clumps do not form unless the disk is highly atypical (e.g., very massive, and hot; *Rafikov*, 2005). Furthermore, unless there are processes acting to keep the disk unstable, weak gravitational instabilities lead to stabilization of the protoplanetary disk via the excitation of spiral density waves (which carry away angular momentum) that spread the disk, lowering its surface density. Given the lack of observational support, along with theoretical arguments against the formation of Jupiter via fragmentation (*Bodenheimer et al.*, 2000; *Cai et al.*, 2006), the gas instability model for Jupiter is not considered viable. For further discussion of the gas instability model, see *Wuchterl et al.* (2000), *Lissauer and Stevenson* (2007), and *Durisen et al.* (2007).

In the core nucleated accretion model (*Pollack et al.*, 1996; *Bodenheimer et al.*, 2000; *Hubickyj et al.*, 2005; *Alibert et al.*, 2005b), Jupiter’s formation and evolution is viewed to occur in the following sequence: (1) Dust particles in the solar nebula form planetesimals that accrete one another, resulting in a solid core surrounded by a low mass gaseous envelope. Initially, runaway accretion of solids occurs, and the accretion rate of gas is very slow. As the solid material in the planet’s feeding zone (the “zone” is defined by the separation distance between a massive planet and a massless body on circular orbits such that they never experience a close encounter; *Lissauer*, 1995) is depleted, the rate of solids accretion tapers off. The gas accretion rate steadily increases

and eventually exceeds the accretion rate of solids. (2) Proto-Jupiter continues to grow as the gas accretes at a relatively constant rate. The mass of the solid core also increases, but at a slower rate. Eventually, the core and envelope masses become equal. (3) Near this point, the rate of gas accretion increases in runaway fashion, and proto-Jupiter grows at a rapidly accelerating rate. The first three parts of the evolutionary sequence are referred to as the *nebular* stage, because the outer boundary of the protoplanetary envelope is in contact with the solar nebula, and the density and temperature at this interface are those of the nebula. (4) The gas accretion rate reaches a limiting value defined by the rate at which the nebula can transport gas to the vicinity of the planet. After this point, the equilibrium region of proto-Jupiter contracts, and gas accretes hydrodynamically into this equilibrium region. This part of the evolution is considered to be the *transition* stage. (5) Accretion is stopped by either the opening of a gap in the gas disk as a consequence of the tidal effect of Jupiter, accumulation of all nearby gas, or by dissipation of the nebula. Once accretion stops, the planet enters the *isolation* stage. Jupiter then contracts and cools to the present state at constant mass. In the following subsections, we present a more detailed summary of this formation sequence.

2.1. From Dust to Planetesimals

Sufficiently far away from the Sun where temperatures are low enough to allow for the condensation of solid material (typically $\gtrsim 0.05$ AU for refractories), grain growth begins with sticking of sub-micron sized dust, composed of surviving interstellar grains and condensates which formed within the protoplanetary disk. These small grains are dynamically coupled to the nebula gas, and collide at low (size-dependent) relative velocities that can be caused by a variety of mechanisms (Völk *et al.*, 1980; Weidenschilling, 1984; Nakagawa *et al.*, 1986; Weidenschilling and Cuzzi, 1993; Ossenkopf, 1993; Cuzzi and Hogan, 2003; Ormel and Cuzzi, 2007). Low impact velocities (and thus low impact energies) tend to allow small particles to grow more efficiently because collisions can be completely inelastic (e.g., Wurm and Blum, 1998). However, as grains collide to form larger and larger agglomerates, the level of coupling between growing particles and the gas decreases, and particle velocities relative to both other particles and the gas increases. As a result, larger particles begin to experience higher impact energies during interparticle collisions which can lead to fragmentation or erosion, in addition to growth.

When the level of coupling between particles and the gas decreases, dust grains, which can be initially suspended at distances well above and below the solar nebula midplane, also begin to gravitationally settle toward the midplane. As particles settle, they may continue to grow. The time it takes for a particle to settle is a function of its size, and may be hundreds, thousands, or more orbital periods depending on ambient nebula conditions. Very small particles (e.g., sub-micron grains) have such long settling times relative to the lifetime of the gas disk that they are considered to be fully “entrained” in the gas. On the other end, some particles may become large enough that their settling time is comparable to their orbital period. These particles tend to have the fastest drift rate relative to the surrounding gas (once they reach this size, the rate decreases again as they grow larger). Although technically these particles couple with the gas once per orbital period, they are essentially viewed as the transition size from a regime in which particles collectively move with the gas (but do so less and less as they grow), to a regime in which particles would prefer to move at the local Kepler orbital speed (but cannot because the gas impedes their motion). These transitional particles are referred to as the “decoupling size”, and as they settle to the nebular midplane they continue to grow by sweeping up dust and rubble (Cuzzi *et al.*, 1993; Weidenschilling, 1997).

The fact that particles tend drift relative to the surrounding gas indicates that the gas component itself does not rotate at the local Kepler orbital velocity, v_K . This is because the nebula gas is not

supported against the Sun’s gravity by rotation alone. In an inertial frame with the Sun at the origin, there are three forces at work at any point on the gas within the nebula disk: a gravitational force radially directed toward the Sun; a centrifugal force directed radially outward from the nebula’s rotation axis; and (because the gas is not pressureless) an outward directed pressure gradient force that works to counter the effective gravity. The condition for hydrostatic equilibrium (although a simplification because the nebula disk is slightly non-Keplerian) then requires that the nebula gas orbit at a velocity slightly less than v_K . Solid objects, which might otherwise orbit at the local orbital speed, are not supported by the pressure gradient, and are thus subject to a drag force that can systematically remove their angular momentum leading to orbital decay (*Weidenschilling, 1977a*).

Thus, a more formal definition of the decoupling size is the size at which the time needed for the gas drag force to dissipate a particles momentum (known as the “stopping time”) is similar to its orbital period. At Jupiter, this size is $R \sim 1$ m (e.g., *Cuzzi et al., 1993*) for the canonical MMSN model. Because decoupling-size particles encounter the strongest drag force, they tend to have the most rapid inward orbital migration. For example, such a particle (assuming no growth) would eventually spiral in to the Sun in $\sim 10^4 - 10^5$ years. This time is rather short compared to planetary accretion timescales ($\gtrsim 10^6 - 10^7$ years); but, as objects grow larger, the drag force on them decreases and the stopping times can become quite long. Kilometer-sized planetesimals are mostly unaffected by the gas due to their greater mass-to-surface-area ratio. Thus quickly getting from meter-sized objects to the safety of relatively immobile ($\gtrsim 1$ km) planetesimals is a key issue in planet formation.

However, whether growth beyond the decoupling size happens depends on the level of turbulence in the disk. This is because collisional velocities for decoupling-size objects can reach tens of meters per second in turbulence, which has more of a tendency to destroy them than promote growth. This suggests that, while the incremental growth of sufficiently small grains and dust may take place irrespective of the level of nebula turbulence, successful growth past the decoupling size may require very low levels of turbulence (e.g., *Youdin and Shu, 2002; Cuzzi and Weidenschilling, 2004*) in order to overcome the two main obstacles for this critical size – collisional disruption, and rapid orbital migration. To this end, several mechanisms have been proposed in the literature to explain planetesimal growth under non-turbulent (laminar) conditions (*Safronov, 1960; Goldreich and Ward, 1973; Weidenschilling, 1997; Sekiya, 1998; Youdin and Chiang, 2004*). Yet, inspite of the difficulties associated with potentially destructive collisions, mechanisms that attempt to explain various stages of planetesimal formation under turbulent conditions have also recently been advanced (see *Cuzzi and Weidenschilling, 2006; Cuzzi et al., 2007; Johansen et al., 2007*).

One may very well conclude from these past and recent works that growth under non-turbulent conditions provides a straightforward pathway to planetesimal formation, while growth in the turbulent regime is a more complicated process with many stages. The greater controversy, however, may be not really so much whether planetesimals can form in turbulence or not, but whether the nebula was turbulent during the epoch of planetesimal to giant planet formation. Indeed, the transition from agglomerates to planetesimals continues to provide the major stumbling block in planetary origins (*Weidenschilling, 1997; 2002, 2004; Weidenschilling and Cuzzi, 1993; Stepinski and Valageas, 1997; Dullemond and Dominik, 2005; Cuzzi and Weidenschilling, 2006; Dominik et al., 2007*).

2.2. Core Accretion

The initial stage of Jupiter’s formation entails the accretion of its solid core from the available reservoir of heliocentric planetesimals that formed as a result of dust coagulation and settling to

the disk midplane. Once planetesimals grow large enough, gravitational interactions between pairs of solid planetesimals provide the dominant perturbation of their basic Keplerian orbits. At this stage, effects that were more influential in the earlier stages of growth such as electromagnetic forces, collective gravitational effects, and in most circumstances gas drag, play minor roles. These planetesimals continue to agglomerate via pairwise mergers, with the rate of solid body accretion by a planetesimal or planetary embryo (basically a very large planetesimal) being determined by the size and mass of the planetesimal/planetary embryo, the surface density of planetesimals, and the distribution of planetesimal velocities relative to the accreting body.

The planetesimal velocity distribution is probably the most important factor that controls the growth rate of planetary embryos into the core of a giant planet. As larger objects accrete, gravitational scatterings and elastic collisions can convert the ordered relative motions of orbiting planetesimals (i.e., Keplerian shear) into random motions, and can “stir up” the planetesimal random velocities up to the escape speed from the largest planetesimals in the swarm (*Safronov*, 1969). The effects of this gravitational stirring, however, tend to be balanced by collisional damping, because inelastic collisions (and gas drag) can damp eccentricities and inclinations especially for the smaller objects.

If one assumes that planetesimal pairwise collisions lead to perfect accretion, i.e., that all physical collisions are completely inelastic (fragmentation, erosion, and bouncing do not occur), this stage of growth can be initially quite rapid (though this is not meant to imply that perfect accretion is needed for rapid growth, however). With this assumption, the planetesimal accretion rate, \dot{M}_Z , is:

$$\dot{M}_Z = \pi R^2 \sigma_Z \Omega F_g, \quad (1)$$

where R is the radius of the accreting body, σ_Z is the surface density of solid planetesimals in the solar nebula, Ω is the orbital frequency at the location of the growing body, and F_g is the gravitational enhancement factor, which in the 2-body approximation (ignoring the tidal effects of the Sun’s gravity) is given by:

$$F_g = 1 + \left(\frac{v_e}{v} \right)^2. \quad (2)$$

Here, v_e is the escape velocity from the surface of the planetary embryo, and v is the velocity dispersion of the planetesimals being accreted. The gravitational enhancement factor F_g arises from the ratio of the distance of close approach to the asymptotic unperturbed impact parameter in a two-body hyperbolic encounter, and can be derived using conservation of angular momentum and energy of the planetesimal relative to the planetary embryo. The evolution of the planetesimal size distribution is determined by F_g , which favors collisions between bodies having larger masses and smaller relative velocities. The largest bodies in the planetesimal swarm (with correspondingly large v_e) have the largest ratio of the total effective accretion cross-section to the geometric cross-section (another way to think of F_g). Moreover, they can accrete almost every planetesimal they collide with (i.e., the perfect accretion approximation works best for the largest bodies).

As the planetesimal size distribution evolves, planetesimals (and planetary embryos) may pass through different growth regimes. These growth regimes are sometimes characterized as either *orderly* or *runaway*. When the relative velocities between planetesimals is comparable to or larger than the escape velocity, $v \gtrsim v_e$, the growth rate \dot{M}_Z is approximately proportional to R^2 . This implies that the growth in radius is roughly constant (as can be easily derived from Eq. 1). Thus the evolutionary path of the planetesimals exhibits an orderly growth across the entire size distribution so that planetesimals containing most of the mass double their masses at least as rapidly as the largest particle. When the relative velocity is small, $v \ll v_e$, the gravitational enhancement factor

$F_g \propto R^2$, and so the growth rate \dot{M}_Z is proportional to R^4 . By virtue of its large, gravitationally enhanced cross-section, the largest most massive embryo doubles its mass faster than the smaller bodies do, and detaches itself from the mass distribution (*Wetherill and Stewart, 1989; Ohtsuki et al., 2002*).

Eventually the runaway body can grow so large (its F_g can exceed ~ 1000) that it transitions from dispersion-dominated growth to shear-dominated growth (*Lissauer, 1987*). This means that for these extremely low random velocities ($v \ll v_e$), the rate at which planetesimals encounter the growing planetary embryo is determined by the Keplerian shear in the planetesimal disk, and not by the random motions of the planetesimals. At this stage, larger embryos take longer to double in mass than do smaller ones, although embryos of all masses continue their runaway growth relative to surrounding planetesimals. This phase of rapid accretion of planetary embryos is known as *oligarchic* growth (*Kokubo and Ida, 1998*).

Rapid runaway or oligarchic accretion requires low random velocities, and thus small radial excursions of planetesimals. The planetary embryo's feeding zone is therefore limited to the annulus of planetesimals which it can gravitationally perturb into embryo-crossing orbits. Rapid growth stops when a planetary embryo has accreted most of the planetesimals within its feeding zone. Thus, runaway/oligarchic growth is self-limiting in nature, which implies that massive planetary embryos form at regular intervals in semimajor axis. The agglomeration of these embryos into a small number of widely spaced bodies necessarily requires a stage characterized by large orbital eccentricities. The large velocities implied by these large eccentricities imply small collision cross-sections (Eq. 2) and hence long accretion times. Growth via binary (pairwise) collisions proceeds until the spacing of planetary orbits become dynamically isolated from one another, i.e., sufficient for the configuration to be stable to gravitational interactions among the planets for the lifetime of the system (*Safronov, 1969; Wetherill, 1990; Lissauer, 1993, 1995; Agnor et al., 1999; Laskar, 2000; Chambers, 2001*).

For shear-dominated accretion, the mass at which such a planetary embryo becomes isolated from the surrounding circumsolar disk via runaway accretion is given by (*Lissauer, 1993*):

$$M_{iso} = \frac{(8\pi\sqrt{3}r^2\sigma_Z)^{3/2}}{(3M_\odot)^{1/2}} \approx 1.6 \times 10^{25} (\sigma_Z r_{AU}^2) \text{ g}, \quad (3)$$

where r_{AU} is the distance from the Sun in astronomical units ($AU = 1.496 \times 10^{13}$ cm). For the MMSN in which only local growth is considered, the mass at which runaway accretion would have ceased in Jupiter's accretion zone is $\sim 1 M_\oplus$ (*Lissauer, 1987*) which is likely too small to explain Jupiter's formation (see below). Runaway accretion can persist beyond the isolation mass if additional solids can diffuse into its feeding zone (thus continued growth is non-local). There are three plausible mechanisms for such diffusion: scattering between planetesimals, perturbations by neighboring planetary embryos, and migration of smaller planetesimals due to gas drag (Sec. 2.1). Other mechanisms that can lead to the migration of embryos from regions that are depleted in planetesimals into regions that are not depleted include gravitational torques resulting from the excitation of spiral density waves in the gaseous component of the disk (see Sec. 4.3.3), and dynamical friction (if significant energy is transferred from the planetary embryo to the protoplanetary disk; e.g., see *Stewart and Wetherill, 1988*).

In the inner part of protoplanetary disks, Kepler shear is too great to allow the accretion of solid planets larger than a few M_\oplus on any timescale unless the surface densities are considerably above that of the MMSN or a large amount of radial migration occurs. However, the fact that the relatively small terrestrial planets orbit deep within the Sun's potential well suggests that they likely were unable to eject substantial amounts of material from the inner Solar System. Thus, the total

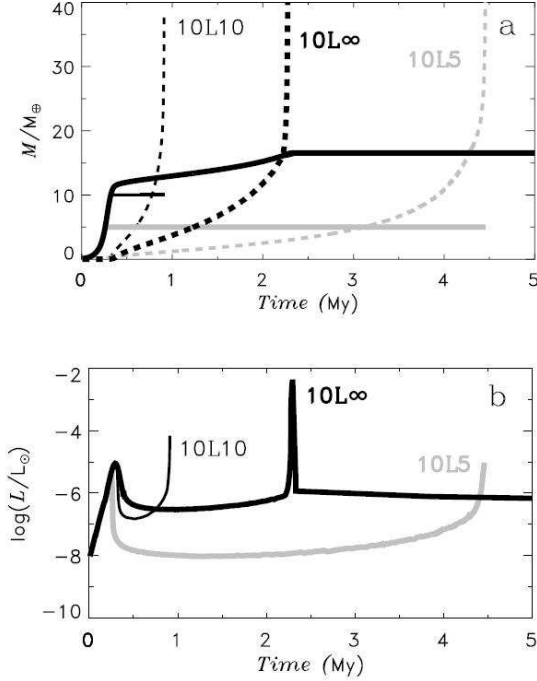


Figure 1: Evolution of a proto-Jupiter with $\sigma_Z = 10 \text{ g cm}^{-2}$ and grain opacity at 2% interstellar value. Details of the calculation are presented in *Hubickyj et al. (2005)*. (a) The mass is plotted as a function of time, with the solid lines referring to the solids component of the planet, the dotted lines to the gaseous component and the dot-dashed lines represent the total mass. *Thick black curves*: no solid accretion cutoff. *Thin black curves*: solid accretion cutoff at $10 M_{\oplus}$. *Gray curves*: solid accretion cutoff at $5 M_{\oplus}$. (b) The luminosity is plotted on a logarithmic scale as a function of time. Note that the cutoff runs are halted when the gas accretion rate reaches a limiting value defined by the rate at which the solar nebula can transport gas to the vicinity of the planet, whereas the planet in the run with no cutoff stops growing when $M_P = 1 M_J$. The existence of a sharp peak in planetary luminosity during the phase of rapid gas accretion is physically plausible, but this peak could be lower and broader than shown in the plot. This calculation assumes that the gas accretion rate is cut off abruptly. Courtesy O. Hubickyj.

amount of mass present in the terrestrial region during the runaway accretion epoch was probably not much more than the current mass of the terrestrial planets, implying that a high-velocity growth phase subsequent to runaway accretion was necessary in order to explain their present configuration (*Lissauer, 1995*).

This high-velocity final growth stage takes $O(10^8)$ years in the terrestrial planet zone (*Safronov, 1969; Wetherill, 1980; Agnor et al., 1999; Chambers, 2001*), but would require $O(10^9 - 10^{10})$ years in the giant planet zone (*Safronov, 1969*) if one assumes local growth in a MMSN disk. These timescales reflect a slowing down of the accretion rate during the late stages of planetary growth due to a drop in the planetesimals surface density (*Wetherill, 1980, 1986*). These growth timescales are far longer than any modern estimates of the lifetimes of gas within protoplanetary disks ($\lesssim 10^7$ years), implying that Jupiter's core must grow large enough during the rapid runaway/oligarchic growth (*Meyer et al., 2007*). The epoch of runaway/rapid oligarchic growth lasts only millions of years or less near the location of Jupiter ($r = 5.2 \text{ AU}$), but can produce $\sim 10 M_{\oplus}$ cores if the circumsolar disk is enhanced in solids by only a few times the MMSN (*Lissauer, 1987*). The limits on the initial surface density of the disk are less restrictive in the giant planet region, because excess solid material can be ejected to the Oort cloud, or out of the Solar System altogether.

The masses at which planets become isolated from the disk thereby terminating the runaway/rapid oligarchic growth epoch are likely to be comparably large at greater distances from the Sun. However, at these large distances, random velocities of planetesimals must remain quite small for accretion rates to be sufficiently rapid for planetary embryos to approach M_{iso} within the lifetimes of gaseous disks (*Pollack et al., 1996*). Indeed, if planetesimal velocities become too large, material is more likely to be ejected to interstellar space than accreted by the planetary embryos.

2.3. Gas Accretion

2.3.1. Tenuous Extended Envelope Phase. As the core grows, its gravitational potential well gets deeper allowing the protoplanet’s gravity to pull gas from the surrounding nebula towards it, and it may begin to accumulate a gaseous envelope. A planet of order one to several M_{\oplus} is able to capture an atmosphere because the escape speed from its physical surface is large compared to the thermal velocity (or sound speed) c_s of the surrounding gaseous protoplanetary disk. Initially, the radial extent of the region in which the gaseous envelope is bound to the protoplanet is determined by the location at which the thermal energy of a gas particle in the solar nebula is greater than the gravitational energy binding it to the planet, and thus it is not bound to the protoplanet (Cameron *et al.*, 1982; Bodenheimer and Pollack, 1986). This is referred to as the accretion radius: $R_A = GM_P/c_s^2$ (G is the gravitational constant). If the protoplanet is small, this bound region can be significantly smaller than the protoplanet’s gravitational domain, whose size is typically a large fraction of the protoplanet’s Hill sphere, R_H , which is given by:

$$R_H = \left(\frac{M_P}{3M_{\odot}} \right)^{1/3} r. \quad (4)$$

Here, M_P is the mass of the protoplanet, and r is the distance between the protoplanet and the Sun. The Hill radius denotes the distance from a planet’s center along the planet-Sun line at which the planet’s gravity equals the tidal force of the solar gravity relative to the planet’s center (Hill, 1878). As the protoplanet increases in mass, the region in which gas can be bound increases and may become a significant fraction of R_H .

An embryo begins to accrete gas slowly, so its gaseous envelope is initially optically thin and isothermal with the surrounding protoplanetary disk; but, as it gains mass it becomes optically thick to outgoing thermal radiation, and its lower reaches can get much warmer and denser than the gas in the surrounding protoplanetary disk. As the protoplanet’s gravity continues to pull in gas from the surrounding disk towards it, thermal pressure from the existing envelope pushes outwards to the limits of the protoplanet’s gravitational reach which can have the effect of limiting further accretion. This is because, for much of its gas accretion stage, the key factor limiting the protoplanet’s accumulation of gas is its ability to radiate away the gravitational energy provided by the continued accretion of planetesimals and the contraction of the envelope; this energy loss is necessary for the envelope to further contract and allow more gas to enter the protoplanet’s gravitational domain.

As the energy released by the accretion of planetesimals and gas is radiated away at the protoplanet’s photosphere, the photosphere cools and a subsequent pressure drop causes the envelope to contract to compensate for the drop in pressure (this is referred to as a Kelvin-Helmholtz contraction). Compression heats the envelope and regulates the rate of contraction which, in turn, controls how rapidly additional gas can enter the planet’s gravitational domain and be accreted.

This suggests that the rate and manner in which a giant planet accretes solids can substantially affect its ability to attract gas. Initially accreted solids form the planet’s core (Sec. 2.2), around which gas is able to accumulate. Calculated gas accretion rates are very strongly increasing functions of the total mass of the protoplanet, implying that rapid growth of the core is a key factor in enabling a protoplanet to accumulate substantial quantities of gas. Continued accretion of solids acts to reduce the protoplanet’s growth time by increasing the depth of its gravitational potential well, but also counters growth by providing additional thermal energy to the envelope from solids that sink to the core. Another hurdle to rapid growth that planetesimal accretion provides is the increased atmospheric opacity from dust grains that are released (ablated) in the upper parts of the envelope. If the opacity is sufficiently high, much of the growing planet’s envelope transports energy via convection. However, the distended very low density outer region of the envelope has

thermal gradients that are too small for convection, but are large enough that they can act as an efficient thermal blanket if it is sufficiently dusty to be moderately opaque to outgoing radiation. This has the effect of slowing contraction and frustrating further accretion of gas, and lengthening the timescale for planet accretion.

Figure 1 shows the evolution of the mass (a) and luminosity (b) for a Jupiter-like planet for three models of giant planet formation. During the runaway planetesimal accretion epoch (when the core is predominantly being formed), the protoplanet’s mass increases rapidly (bold solid curve). Although at this point the gaseous atmosphere is quite tenuous (dashed curves), the internal temperature and thermal pressure of the envelope increases, which prevents substantial amounts of nebular gas from falling onto the protoplanet. When the rate of planetesimal accretion decreases (roughly around $M_P \gtrsim 10 M_\oplus$), gas falls onto the protoplanet more rapidly as the additional component of thermal energy contributed by the accreting planetesimals decreases. At this stage the envelope mass is a sensitive function of the total mass, with the gaseous fraction increasing rapidly as the planet accretes (*Pollack et al.*, 1996). Eventually, increases in the planet’s mass and the radiation of energy allow the envelope to shrink rapidly. When the envelope reaches a mass comparable to that of the core, the self-gravity of the gas becomes substantial, and the envelope contracts when more gas is added. Further accretion is then governed by the availability of gas rather than thermal considerations. At this point, the factor limiting the planet’s growth rate is the flow of gas from the surrounding protoplanetary disk.

The time required to reach this stage of rapid gas accretion is governed primarily by three factors: the mass of the solid core (a larger core mass implies more rapid gas accretion); the rate of energy input from continued accretion of solids (such energy keeps the envelope large and slows further accretion of gas); and the opacity of the envelope (low opacity allows the radiation of energy that enables the envelope to cool and shrink, making room for more gas to be accreted). These three factors appear to be key in determining whether giant planets are able to form within the lifetimes of protoplanetary disks ($\lesssim 10^7$ years). For example, in a disk with initial $\sigma_Z = 10 \text{ g cm}^{-2}$ at 5.2 AU from a $1 M_\odot$ star, a planet whose atmosphere has 2% interstellar opacity (i.e., $\sim 0.02 \text{ cm}^2 \text{ g}^{-1}$) forms with a $16 M_\oplus$ core in 2.3 Myr; in the same disk, a planet whose atmosphere has full interstellar opacity ($\sim 1 \text{ cm}^2 \text{ g}^{-1}$) forms with a $17 M_\oplus$ core in 6.3 Myr; a planet whose atmosphere has 2% interstellar opacity but stops accreting solids at $10 M_\oplus$ forms in 0.9 Myr, whereas if solids accretion is halted at $3 M_\oplus$ accretion of a massive envelope requires 12 Myr (*Hubickyj et al.*, 2005). These results suggest that if Jupiter’s core mass is significantly less than $10 M_\oplus$, then it presents a problem for formation models mainly because disk dispersal times are observed to be shorter than the time it takes for a smaller core mass to accrete a massive enough envelope (unless the opacity of the envelope to outgoing radiation is significantly less than 2% of the interstellar medium).

Thus, the key to forming Jupiter prior to the dispersal of the nebula is the rapid formation of a massive core coupled with a combination of a decreased solids accretion rate and/or the outer regions of the giant planet envelope being transparent to outgoing radiation. However, since there is little in the way of observational constraints, our understanding continues to be handicapped by uncertainties in quantities such as the opacity and solids accretion rate that are derived from planet formation models. One constraint that may provide some insight, however, is the composition of the atmosphere of the giant planets which is presumed to be largely determined by how much heavy material was mixed with the lightweight material in the planet’s envelope. As the envelope becomes more massive, late-accreting planetesimals (but, early-arriving in the context of satellite formation, see Sec. 4) sublime before they can reach the core, thereby enhancing the heavy element content of the envelope considerably. In Sec. 2.4, we discuss more on the composition of Jupiter’s envelope.

2.3.2. Hydrodynamic Phase. As we saw demonstrated in Fig. 1, a protoplanet accumulates gas

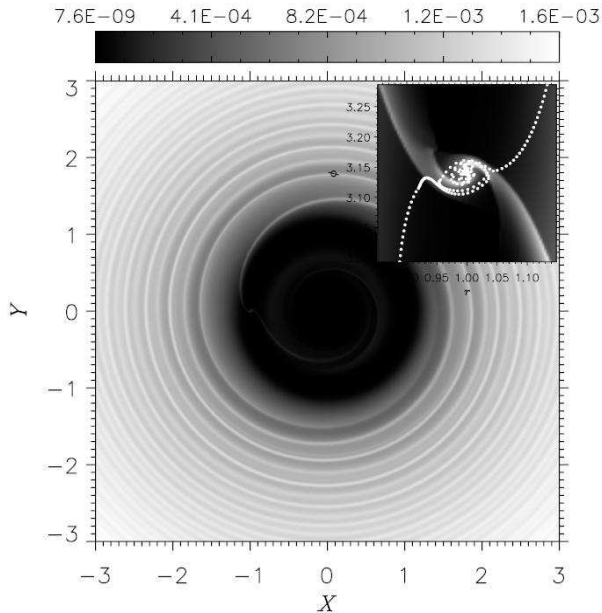


Figure 2: The surface mass density of a gaseous disk containing a Jupiter-mass planet on a circular orbit located 5.2 AU from a $1 M_{\odot}$ star. The ratio of the scale height of the disk to the distance from the star is $1/20$, and the dimensionless viscosity at the location of the planet is $\alpha = 4 \times 10^{-3}$. The distance scale is in units of the planet’s orbital distance, and surface density of 10^{-4} corresponds to 33 g cm^{-2} . The inset shows a close-up of the disk region around the planet, plotted in cylindrical coordinates. The two series of white dots indicate actual trajectories (real particle paths, not streamlines) of material that is captured in the gravitational well of the planet and eventually accreted by the planet. See *D’Angelo et al.*, (2005) for a description of the code used.

at a gradually increasing rate until its gas component is comparable to its heavy element mass (i.e., the envelope and core are of comparable mass). At this point, the protoplanet has enough mass for its self-gravity to compress the envelope substantially. The rate of gas accretion then accelerates rapidly, and a gas runaway occurs (*Pollack et al.*, 1996; *Hubickyj et al.*, 2005). This accretion continues as long as there is gas in the vicinity of the protoplanet’s orbit. Indeed, it is found that the ability of the protoplanet to accrete gas does not depend strongly on the outer boundary conditions (temperature and pressure) of the surrounding nebula, if there is adequate gas around to be accreted (*Mizuno*, 1980; *Stevenson*, 1982; *Pollack et al.*, 1996). Hydrodynamic limits allow quite rapid gas flow to the planet in an unperturbed disk. But in realistic scenarios, the protoplanet not only alters the disk by accreting material from it, but also by exerting gravitational torques on it (see Sec. 4). Both of these processes can lead to a formation of a gap in the circumsolar gas disk (e.g., *Lin and Papaloizou*, 1979) and isolation of the planet from the surrounding gas, thus providing a means of limiting the final mass of the giant planet.

Observationally, such gravitationally induced gaps (in solids) have been observed around small moons within Saturn’s rings (*Showalter*, 1991; *Porco et al.*, 2005). Numerically, gas gap formation has been studied extensively. For example, *D’Angelo et al.*, (2003b) used a 3D adaptive mesh refinement code to follow the flow of gas onto accreting giant planets of various masses embedded within a gaseous protoplanetary disk. *Bate et al.*, (2003) have performed 3D simulations of this problem using the ZEUS hydrodynamics code. Using parameters appropriate for a moderately viscous MMSN protoplanetary disk at 5 AU, both groups found that $< 10 M_{\oplus}$ planets don’t perturb the protoplanetary disk enough to significantly affect the amount of gas that flows towards them. Gravitational torques on the disk by larger planets under these disk conditions drive away gas. In a moderately viscous disk, hydrodynamic limits on gas accretion reach to a few $\times 10^{-2} M_{\oplus}$ per year for planets in the $\sim 50 - 100 M_{\oplus}$ range, and then decline as the planet continues to grow. An example of gas flow around/to a $1 M_J$ planet is shown in Figure 2. In general, caution must be exercised in the interpretation of these types of calculations when attempting to connect them with the formation of the giant planet itself. Thus, for example, these calculations do not

include the thermal pressure on the nebula from the hot planet, which is found to be the major accretion-limiting factor for planets up to a few tens of M_{\oplus} by the simulations discussed in Section 2.3.1 (*Hubickyj et al.*, 2005; *Lissauer and Stevenson*, 2007). It should further be noted that ability for a protoplanet to push gas away from itself is very much dependent on the viscosity of the disk. In nearly inviscid disks, for example, a $\sim 10 M_{\oplus}$ protoplanet may be capable of pushing gas away from itself (*Rafikov*, 2002a,b; Sec. 4.3.3).

If the planet successfully cuts off its supply of gas by the opening of a gas gap in the circumsolar disk, the planet effectively enters the isolation stage. Jupiter then contracts and cools to its present state at constant mass.

2.4. The Composition of Jupiter’s Envelope

2.4.1. Enhancement in Heavy Elements. The abundances of elements in Jupiter’s atmosphere that are quite volatile, but unlike H and He still condensible within the giant planets of the solar nebula, are about $\sim 3 - 4$ times solar (*Atreya et al.*, 1999; *Mahaffy et al.*, 2000; *Young*, 2003). If the relative abundances of all condensible elements in Jupiter’s envelope are the same as in the Sun, then such material must account for $\sim 18 M_{\oplus}$ (*Owen and Encrenaz*, 2003). This suggests that such solid material must have been abundant in the early Solar System. However, present day evidence for this material remains elusive, because no solid objects (e.g., comets, asteroids) have been found that have solar ratios of Ar, Kr, Xe, S and N relative to C, as does Jupiter.

Explanation for this enhancement has been attributed to one of two different mechanisms. The first idea relies on the delivery of volatiles from the outer regions of the solar nebula that were trapped in amorphous ice and then incorporated into planetesimals. Based on the laboratory work of *Bar-Nun et al.* (1988; also see 2007), this approach initially led to the expectation that Jupiter may not be enhanced in volatile elements like Ar which condenses at very low temperatures (< 30 K) because planetesimals that formed near the snow line likely dominated the delivery of heavy elements to Jupiter’s envelope. A second view for Jupiter’s enhancement proposed by *Gautier et al.* (2001a,b; also cf. *Hersant et al.*, 2004), is that volatiles were trapped in crystalline ices in the form of clathrate-hydrates (*Lunine and Stevenson*, 1985) at different temperatures in Jupiter’s feeding zone which were then incorporated into the planetesimals that went into Jupiter. A problem with the model of *Gautier et al.* (2001b) is that clathration of Ar requires very low solar nebula temperatures $T \sim 36$ K, which is inconsistent with temperatures at Jupiter’s location even using cool passive disk models (*Chiang and Goldreich*, 1997; *Sasselov and Lecar*, 2000).

Given that Ar does not condense at temperatures higher than 30 K, one might expect that the ratio of Ar to H in Jupiter should be the same in Jupiter as the Sun, if indeed Jupiter’s formation were characterized by local growth (see discussion at beginning of Sec. 2). However, there likely was considerable migration of solids due to gas drag in the outer solar nebula (see Figure 3), so it cannot be assumed that material (of solar proportions) remained at the location in the protoplanetary disk where it condensed. This argument is bolstered by high-resolution submillimeter continuum observations that indicate the average dust disk sizes around T Tauri stars are ≈ 200 AU (*Andrews and Williams*, 2007), with similar results being obtained via millimeter interferometry (*Kitamura et al.*, 2002). Furthermore, some gas disks around young stars show flat density distributions (*Dutrey et al.*, 1996; *Wilner et al.*, 2000), suggesting that a significant fraction of the mass of the disk is located at large distances from the star. This dust disk eventually shrinks (even if the gas disk spreads outwards) due to coagulation with objects eventually growing large enough to decouple from the gas and migrate (Sec. 2.1). The initial stages of this evolution take place at sufficient distances that the circumsolar disk is very cold (see Fig. 3), perhaps cold enough to allow for the trapping of volatiles in either amorphous or crystalline (in the form of clathrates) ice, depending

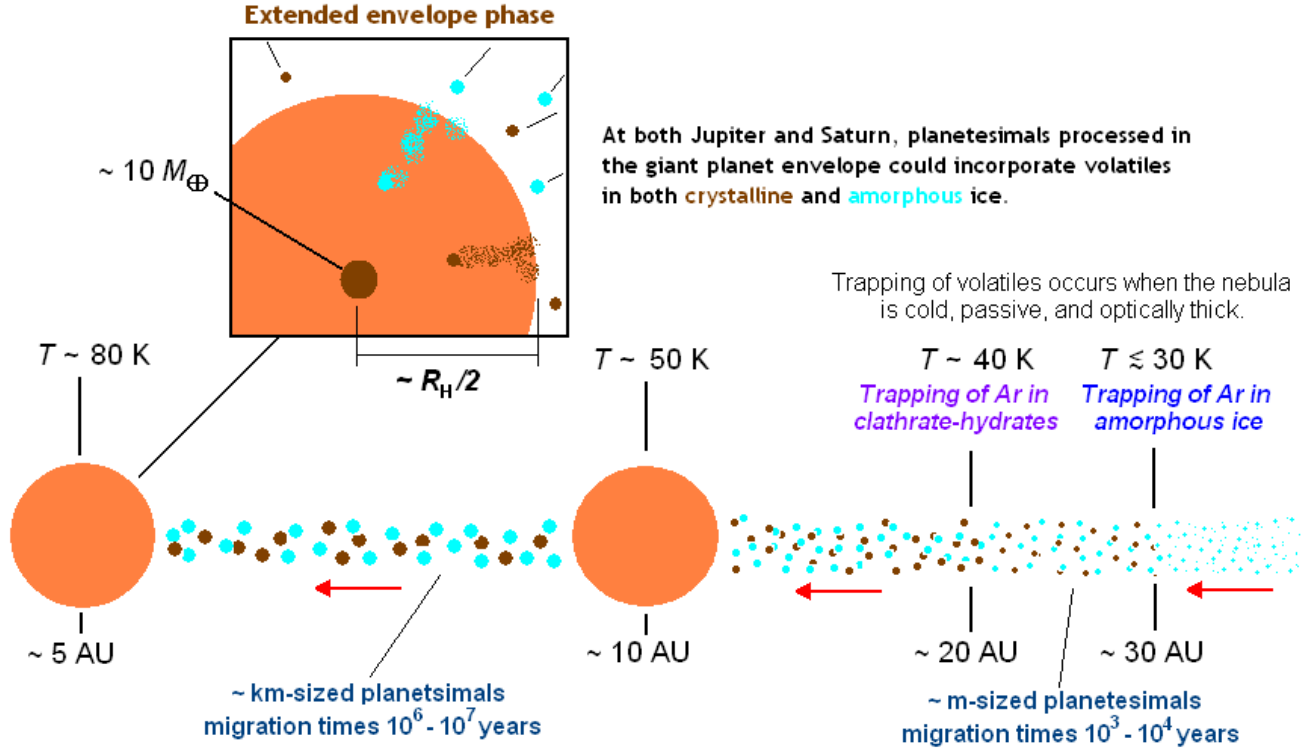


Figure 3: Sufficiently far from the Sun ($\sim 30 \text{ AU}$), amorphous ice forming at low temperatures ($\lesssim 30 \text{ K}$) can trap volatiles (*Owen et al.*, 1999). In warmer regions of the nebula closer to the Sun, ice is crystalline and volatiles may be trapped in clathrate hydrates (*Lunine and Stevenson*, 1985; *Gautier et al.*, 2001a,b). Planetesimals that form in cold regions and cross into warmer regions suffer a transition from amorphous to crystalline ice at a rate that depends on temperature (*Schmitt et al.*, 1989; *Mekler and Podolak*, 1994). The condition that this transition takes longer than the lifetime of the nebula defines a location outside of which amorphous ice can mix in provided cold planetesimals are delivered by gas drag migration in a similar timescale (which applies to planetesimals $< 1 \text{ km}$ for a MMSN). An ice grain may retain its amorphous state for the age of the solar nebula ($\sim 10^7 \text{ years}$) provided that the temperature is $< 85 \text{ K}$. Thus, it may be possible to deliver volatiles to the atmospheres of the forming giant planets either in amorphous ice or crystalline ice, depending on trapping efficiency in the two ice-phases, the initial distribution of mass in the primordial nebula, and the specifics of the growth, migration and thermal evolution of planetesimals. This point of view provides a natural fit for the existence of a Kuiper Belt cut-off – that is, primordial planetesimals located outside $\sim 30 \text{ AU}$ may have migrated to the inner Solar System by gas drag, delivering volatiles and enhancing the solid fraction in the planetary region (this cut-off location refers to the time prior to the outward migration of Neptune, which could have pushed the Kuiper Belt out; *Levison and Morbidelli*, 2003). Note that the temperature chosen at the location of Jupiter and Saturn is consistent with passive disk models (*Chiang and Goldreich*, 1997).

on the trapping efficiency. As these planetesimals drift in, they likely encounter warmer regions. Further growth to even comet sizes $\sim 1 \text{ km}$ occurs at some point (*Weidenschilling*, 1997; *Kornet et al.*, 2004), at which time they attain drag times comparable to the lifetime of the circumsolar gas disk ($\lesssim 10^7 \text{ years}$).

The success of this solids migration mechanism depends on whether inwardly migrating planetesimals that possibly included amorphous ice at the outset (*Mekler and Podolak, 1994*), were altered by the higher temperatures of the inner nebula and became mostly crystalline, losing the volatiles that would have been trapped in them (*Bar-Nun et al., 1985, 1987*). Amorphous ice undergoes a transformation to crystalline ice at a rate that depends strongly on temperature (*Schmitt et al., 1989; Kouchi et al., 1994; Mekler and Podolak, 1994*). An ice grain may retain its amorphous state for the lifetime of the nebula ($\lesssim 10^7$ years) provided the temperature is less than < 85 K. That is, low temperatures favor the preservation of amorphous ice, while long time spans and even temporary elevated temperatures drive the ice toward crystallization.

Thus, while the temperature constraint for incorporation of Ar is quite stringent, the temperature constraint for planetesimals to *preserve* volatiles they acquired in cold portions of the disk may be much less so. Indeed, a temperature of < 85 K is quite consistent with cool passive disk models at the location of Jupiter (*Chiang and Goldreich, 1997*). One potential difficulty that could hinder the effectiveness of this mechanism may depend on whether such planetesimals incorporated significant amounts of short-lived radionuclides such as ^{26}Al , which would further complicate the ability for planetesimals to preserve their amorphous state (*Prialnik and Podolak, 1995*). Nevertheless, in the outer disk one would naturally expect longer accretion times, which would result in weaker radioactive heating and lower temperatures. However, it remains to be shown whether one can expect amorphous ice to be preserved in migrating planetesimals over the lifetime of the solar nebula, which might make it possible for delivery of Ar to Jupiter.

2.4.2. The Snow Line and Planetesimal Delivery. A likely consequence of this picture is that a shrinking (dust) disk would lead to a higher solids fraction in the planetary region than given by the MMSN. As we noted in Sec. 2.2, this is consistent with the requirement that the circumsolar disk be enhanced in solids by at least a factor of few in order for $\sim 10 M_{\oplus}$ cores to be produced during the runaway/oligarchic growth phase. Subsequently, much of the “excess” material, variously estimated between $50 - 100 M_{\oplus}$ (*Stern, 2003; Goldreich et al., 2004*), may wind up in the Oort cloud. Since Earth-sized objects may migrate (not via gas drag, but by mutual gravitational interaction with the gaseous disk, see Sec. 4.3.3) in a time shorter than or comparable to the nebula dissipation time, some of this solid material may be lost to the Sun.

On the other hand, meter-sized objects have relatively short gas drag migration times ($\sim 10^4 - 10^5$ years at Jupiter), so it is possible that some fraction of the solid content of the disk drifted in until it encountered the snow line (i.e., that location outside of which water-ice may condense). Inwardly drifting planetesimals then might sublimate at this (water-ice) evaporation front (*Cuzzi et al., 2003; Cuzzi and Zahnle, 2004; Ciesla and Cuzzi, 2006*). Within the context of the model proposed by these workers, the snow line might receive most of the volatile enhancement, even for heavy elements more volatile than water. If the solar nebula were turbulent, then diffusion due to turbulence might spread the effects of this evaporation front over a larger region. Typically, the snow line is thought to be somewhere between $3 - 5$ AU (*Morfill and Völk, 1984; Stevenson and Lunine, 1988; Cuzzi and Zahnle, 2004*), so that one might then be led to expect that the volatile heavy element enrichment in Jupiter’s envelope is due to the high-volatile content of the nebula at its location. This scenario would imply that the enrichment in Jupiter should be more pronounced than Saturn’s. Yet this conclusion appears to be in conflict with the Saturn’s elemental ratio with respect to solar of C/H ($\sim 2 - 6$, *Courtin et al., 1984; Buriez and de Bergh, 1981*) and N/H ($\sim 2 - 4$, *Marten et al., 1980; de Pater and Massie, 1985*). However, the enhancement at the water-ice evaporation front would still be dependent on how much of this material is delivered and in what state it reaches the Jupiter region. Moreover, delivery of volatiles via planetesimals may be a more efficient process. Thus, it is presently unclear whether it is possible to deliver and enhance

heavy elements more volatile than water simultaneously at Jupiter (and Saturn) by enriching the nebula gas instead of direct planetesimal delivery, which would likely predict a *higher* heavy element enhancement for planets that accreted *less* gas from the nebula.

3. FORMATION OF THE CIRCUMJOVIAN DISK

As Jupiter’s core mass grows, it obtains a substantial atmosphere through the collection of the surrounding solar nebula gas. Early on (still in the nebular stage), this gas falls onto a distended envelope that extends out to a significant fraction of the Hill sphere. Later, roughly around the time that the core mass and envelope mass are equivalent, the protoplanet undergoes runaway gas accretion. Once the protoplanet reaches a mass of $\sim 50 - 100 M_{\oplus}$, the envelope contracts rapidly (transition stage). Eventually, Jupiter becomes massive enough to truncate the gas disk by the opening of a deep gas gap in the solar nebula and/or because all of the gas in its feeding zone is depleted. At this point accretion ends (isolation stage). We now address how the circumplanetary gas disk fits into this multi-stage process.

3.1. Introduction

A very basic characteristic of the circumjovian disk is its radial extent: how far does it extend from the planet? The answer is that the size of the subnebula depends on the specific angular momentum of gas flowing into the giant planet’s gravitational domain (*Lissauer, 1995; Mosqueira and Estrada, 2003a*). Before and during much of the runaway gas accretion phase of Jupiter’s formation (which spans a period prior to, and after envelope contraction), the gas that enters the protoplanet’s Roche lobe (equivalently, its Hill sphere, see Eq. 4) has low specific angular momentum. This is because the mass of the protoplanet for much of this period is not sufficient to open a significant gas gap in the solar nebula for typical circumsolar disk model parameter choices (see Sec. 3.4, and below). As a result, most of the gas being accreted during this period originates within the vicinity of the protoplanet ($\lesssim R_H$). Prior to envelope contraction, gas accretes onto the giant planet’s distended atmosphere. However, a simple calculation (see Sec. 3.2) indicates that a fraction of this gas has too much rotational angular momentum to collapse down to an object the size of Jupiter (similar arguments are made in the context of star formation from collapsing molecular clouds). Instead, the excess gas falls onto a rotationally supported compact disk.

The contraction of the distended envelope happens early during the runaway gas accretion phase. Current models have Jupiter contracting prior to reaching $\sim 1/3$ of its final mass, and probably well before this. Moreover, the timescale for envelope collapse (down to a few planetary radii) is relatively quick compared to the runaway gas accretion epoch, which lasts $\sim 10^4 - 10^5$ years (see Fig. 1a, *Hubickyj et al., 2005*). This indicates that the subnebula begins to form relatively early in the planet formation process when the planet is not sufficiently large to truncate the gas disk. As a result, the gas that continues to flow into the Roche lobe has mostly low specific angular momentum. Since the proto-Jupiter must still accrete in excess of $\gtrsim 200 M_{\oplus}$ after envelope collapse, it suggests that the gas mass deposited over time in the relatively compact subnebula could be substantial. Furthermore, this picture is consistent with the view that the planet and disk may end up with similar amounts of angular momentum (e.g., *Stevenson et al., 1986; Sec. 4*).

As the protoplanet grows more massive, it more readily perturbs the surrounding nebula gas through the actions of gas accretion and tidal interaction, leading to the formation of a gas gap in the solar nebula (Sec. 2.3.2). Sufficiently massive objects may actually truncate the disk (we will refer to this truncation as a deep gap), which we take to mean that almost all of the available gas in the vicinity of the giant planet has been accreted or pushed away. In a moderately viscous disk, a Jupiter mass planet ($1 M_J$), truncates the disk in a few hundred orbital periods (or $\sim 10^3$ years at

5.2 AU). Larger masses are required to open a deep gap in a viscous disk in order to overcome the tendency of turbulent diffusion to keep the gap full. In addition, because the tidal torque strength depends on the square of the mass of the perturbing body, it may be that disk truncation occurs closer to the tail end of runaway gas accretion phase as Jupiter approaches its final mass.

This picture applies to an accretion scenario for Jupiter that assumes that no other planets influence the evolution of the nebula gas. In a scenario in which the giant planets of the Solar System start out much closer to each other and subsequently migrate outwards (*Tsiganis et al.*, 2005), Saturn would push gas into Jupiter’s gap and vice-versa, and jointly open a gap. In such a scenario, Saturn’s influence would dominate over that of turbulence in a moderately viscous disk.

The process of gap-opening in the circumsolar gas disk has direct bearing on the satellite formation environment because, as the gas gap becomes deeper, the continued gas inflow through this gap can significantly alter the properties of the subnebula. In particular, as gas in the protoplanet’s vicinity is depleted, the inflow begins to be dominated by gas with specific angular momentum which is much higher than what previously accreted onto the distended envelope and/or compact disk. This is because the gas must now come from farther away ($\gtrsim R_H$). Since satellite formation is expected to begin near this time (see Sec. 4), the character of the gas inflow during the waning stage of Jupiter’s accretion is a key issue in determining the environment in which the Galilean satellites form.

It is worth noting that Europa and the other Galilean satellites occupy a compact region (roughly $\sim 4\%$ of the Hill radius). The angular momentum of outermost Callisto is comparable to that of Ganymede (owing to Callisto’s large mass). This similarity in angular momentum of these two Galilean satellites is puzzling since one might expect the outermost satellite to have significantly *less* angular momentum. This is because it is *a priori* difficult to envision how the surface density of the satellite disk could have been large enough to make a massive satellite such as Callisto at its location, but insufficient to form other, smaller satellites outside its orbit (*Mosqueira and Estrada*, 2003a). Callisto’s large mass most likely indicates that the circumjovian disk extended significantly beyond Callisto’s orbit; thus, the lack of regular satellites outside Callisto requires explanation.

Until recently, numerical models that simulate gas accretion onto a “giant planet” embedded in a circumstellar disk could not resolve scales smaller than $\sim 0.1 R_H$ (e.g., *Lubow et al.*, 1999; *Bate et al.*, 2003), a region several times larger than is populated by the regular satellites. It is only with the advent of higher resolution 2D and 3D simulations (described in Sec. 3.3) that it became possible to resolve structure on the scale of the radial extent of the Galilean satellites. These recent simulations indicate that the circumplanetary disk formed by the gas inflow through the gap – irrespective of any subsequent viscous evolution and spreading – likely extended as much as ~ 5 times the size of the Galilean system (*D’Angelo et al.*, 2003b). Thus the specific angular momentum of gas inflow through a gap is significantly larger than that of the satellites themselves.

3.2. Analytical Estimates of Disk Sizes

We can obtain an estimate of the characteristic disk size formed by the accretion of low specific angular momentum gas (and thus it is implicitly assumed that no gap is present), using angular momentum conservation. Assuming that Jupiter travels on a circular orbit, that the solar nebula gas moves in Keplerian orbits, and that *prior* to gap-opening Jupiter accretes gas parcels with semimajor axes originating from up to $1R_H$ of its location, then the specific angular momentum ℓ of the accreted gas is approximately given by (*Lissauer*, 1995):

$$\ell \approx -\Omega \frac{\int_0^{R_H} \frac{3}{2} x^3 dx}{\int_0^{R_H} x dx} + \Omega R_H^2 \approx \frac{1}{4} \Omega R_H^2. \quad (5)$$

The expression for the specific angular momentum estimate given above has two contributions. The first term is the specific angular momentum flux flowing into the planet due to Keplerian shear computed in the frame rotating at the planet’s angular velocity. The second contribution is a correction to translate back to an inertial frame (see *Lissauer, 1995* and references therein). Equation (5) neglects the gravitational effect of the planet, and assumes that the angular momentum of the inflowing gas is delivered to the Roche lobe of the giant planet. Assuming conservation of angular momentum, balancing centrifugal and gravitational forces $\ell^2/r_c^3 \approx GM_J/r_c^2$ allows us to obtain what is referred to as the centrifugal radius (*Cassen and Pettibone, 1976; Stevenson et al., 1986; Lissauer, 1995; Mosqueira and Estrada, 2003a*):

$$r_c \approx R_H/48. \quad (6)$$

For a fully grown Jupiter, the centrifugal radius is located at $r_c \approx 15 R_J$ (where $R_J = 71492$ km is a Jupiter radius) just outside the position of Ganymede (for Saturn, r_c lies just outside of Titan, see Fig. 1 of *Mosqueira and Estrada, 2003a*). The disk size associated with the accretion of low specific angular momentum gas is thus consistent with the radial extent of the Galilean satellites.

On the other hand, *after* gap-opening accretion may continue through the planetary Lagrange points, as seen in some simulations (e.g., *Artymowicz and Lubow, 1996; Lubow et al., 1999*). Specifically, accretion occurs through the L_1 and L_2 points, which are located at roughly a distance R_H from the planet, and along the line connecting protoplanet and Sun (see Fig. 4). At the Lagrange points, the gravitational fields of both the protoplanet and the Sun combined with the centrifugal force are balanced. So as seen in the rotating frame, a massless body placed at this location would have zero relative velocity, and thus be stationary. In this case, the gravitational effects of the planet cannot be neglected – otherwise accretion would cease, as gas parcels would no longer cross the gravitational sphere of influence of the planet. We can obtain an estimate of the specific angular momentum of the gas as it passes through the Lagrange points by assuming that the inflow takes place at a low velocity in the rotating frame and it is directed nearly towards the planet. This may be done by keeping only the change of frame contribution of Eq. (5) or $\ell \sim \Omega R_H^2$. Again, using conservation of angular momentum, the estimated characteristic disk size formed by the inflow is significantly larger than before, roughly $\sim R_H/3 \sim 260 R_J$ (e.g., *Quillen and Trilling, 1998; Mosqueira and Estrada, 2003a*).

These estimates indicate that gas flowing through a gap in the circumsolar disk brings with it significantly higher specific angular momentum, which produces a larger characteristic circumplanetary disk size, than does incoming gas when no gap is present. This information combined with the observed mass distribution of the regular satellites of Jupiter (and Saturn) can be used to argue in favor of a two-component circumplanetary disk: (1) a compact, relatively massive disk that forms over a period of time post envelope collapse and prior to disk truncation, and (2) a more extended, less massive outer disk that forms from gas flowing through a gap and at a lower inflow rate (e.g., *Bryden et al., 1999; D’Angelo et al., 2003b*). An idealization of this two-component subnebula is shown in Fig. 8 (see left panel and caption). However, the details of the formation of the giant planet from the envelope collapse phase, to gap-opening and isolation remains to be shown using hydrodynamical simulations. This is because numerical simulations of giant planet formation tend either to treat the growth of the protoplanet in isolation (e.g., *Pollack et al., 1996; Hubickyj et al., 2005*; see Sec. 2), or to treat giant planets ($\sim 1 M_J$) embedded in circumstellar disks in the presence of a well-defined, deep gap (e.g., *Lubow et al., 1999; Kley 1999; Bate et al., 2003; D’Angelo et al., 2003b*). Mainly because of the computational demands, the latter simulations do not model changing planetary or nebula conditions. Not surprisingly then, the transition between a distended planetary envelope and a thin disk has received scant attention.

A consequence of continued gas inflow through the gap is that the subnebula will continue to evolve due to a turbulent viscosity ν generated by gas accretion onto the circumplanetary disk. In general, the dissipation of viscous energy leads to the transport of mass inwards (facilitating further accretion onto the planet) and angular momentum outwards (causing the disk to spread). The efficiency of the mechanism of angular momentum transport is most commonly characterized by a turbulent parameter $\alpha \propto \nu$, as was suggested in a seminal paper by *Shakura and Sunyaev* (1973). However, even weak values of α can pose a problem for planetesimal formation (Sec. 2.1). The turbulent circumplanetary disk environment generated by the inflow likely means that satellite formation does not begin until late in the planetary formation sequence when the gas inflow (through the gap) wanes, at which point turbulence in the subnebula may decay. The formation of the satellites at the stage where the planet approaches its final mass is further supported by the fact that even weak, ongoing inflow through the gap can generate a substantial amount of heating due to turbulent viscosity, which would generally result in a circumplanetary disk that is too hot for ice to condense and satellites to form and survive (e.g., *Coradini et al.*, 1989; *Makalkin et al.*, 1999; *Klahr and Kley*, 2006). As a result, a very low gas inflow rate – orders of magnitude lower than the accretion rates through gas gaps in numerical simulations ($\sim 10^{-2} \text{ M}_{\oplus} \text{ yr}^{-1}$, e.g., *Lubow et al.*, 1999) – is likely a requirement for the basis of any satellite formation model. Nevertheless, some applicable conclusions can be drawn from existing simulations.

3.3. Numerical Results in 2D/3D in the Presence of a Gap

Two-dimensional hydrodynamics calculations of a Jupiter-mass planet embedded in a circumstellar disk show prograde circulation of material within the planet’s Roche lobe that is reminiscent of a circumplanetary disk (*Lubow et al.*, 1999, *Kley*, 1999). These simulations show that gas can flow through the gap formed by the giant planet, depending on the value for the nebula turbulence parameter ($\alpha \gtrsim 10^{-4}$, *Bryden et al.*, 1999). A prominent feature exhibited in these Roche-lobe flows or streams is a two-arm spiral wave structure (see left panels of Fig. 4, which is a 3D simulation). As gas flow enters the Roche lobe near the planetary Lagrange points, these streams encircle the planet and impact one another on the opposite side (from which they entered). The resulting collision shocks the material, and deflects the flow towards the planet (e.g., *D’Angelo et al.*, 2002). In 2D, the spiral wave structure is weaker (not as tightly wound) for decreasing protoplanet mass, and disappears altogether for $\sim 1 \text{ M}_{\oplus}$ protoplanetary masses. In 3D simulations, these spiral waves are also less marked than in 2D as a consequence of the flow no longer being restricted to a plane (see *D’Angelo et al.*, 2003a). Gas accretion rates in both 2D and 3D are qualitatively similar.

Detailed simulations of such systems pose a significant challenge from a numerical point of view since they demand that both the circumstellar disk and the hydrodynamics deep inside the planet’s Roche lobe must be resolved. This requirement means that length scales must be resolved over more than two orders of magnitude, from the planet’s orbital radius, r_p , down to a few per cent of the Hill radius, R_H . *D’Angelo et al.* (2002, 2003b) carry out a quantitative analysis of the properties of circumplanetary disks around Jovian and sub-Jovian mass planets. By treating the subsystem as a locally isothermal and viscous fluid, and using a grid refinement technique, known as “nested grids” that allow them to resolve length scales around the planet on the order of $0.01 R_H$ ($\sim 7 R_J$ for 1 M_J), these authors are able to show that the dynamical properties of the material orbiting within a few tenths of R_H from the planet are indeed consistent with a disk in Keplerian rotation.

Figure 4 shows the mass density distributions from a three-dimensional, local isothermal model (see *D’Angelo et al.*, 2003b for details). The temperature at 5.2 AU is assumed to be $T \simeq 110 \text{ K}$ (if the mean molecular weight of the gas is about 2.2) and the kinematic viscosity, ν , in this case is assumed to be constant in space and time, and thus not parameterized by a turbulent coefficient

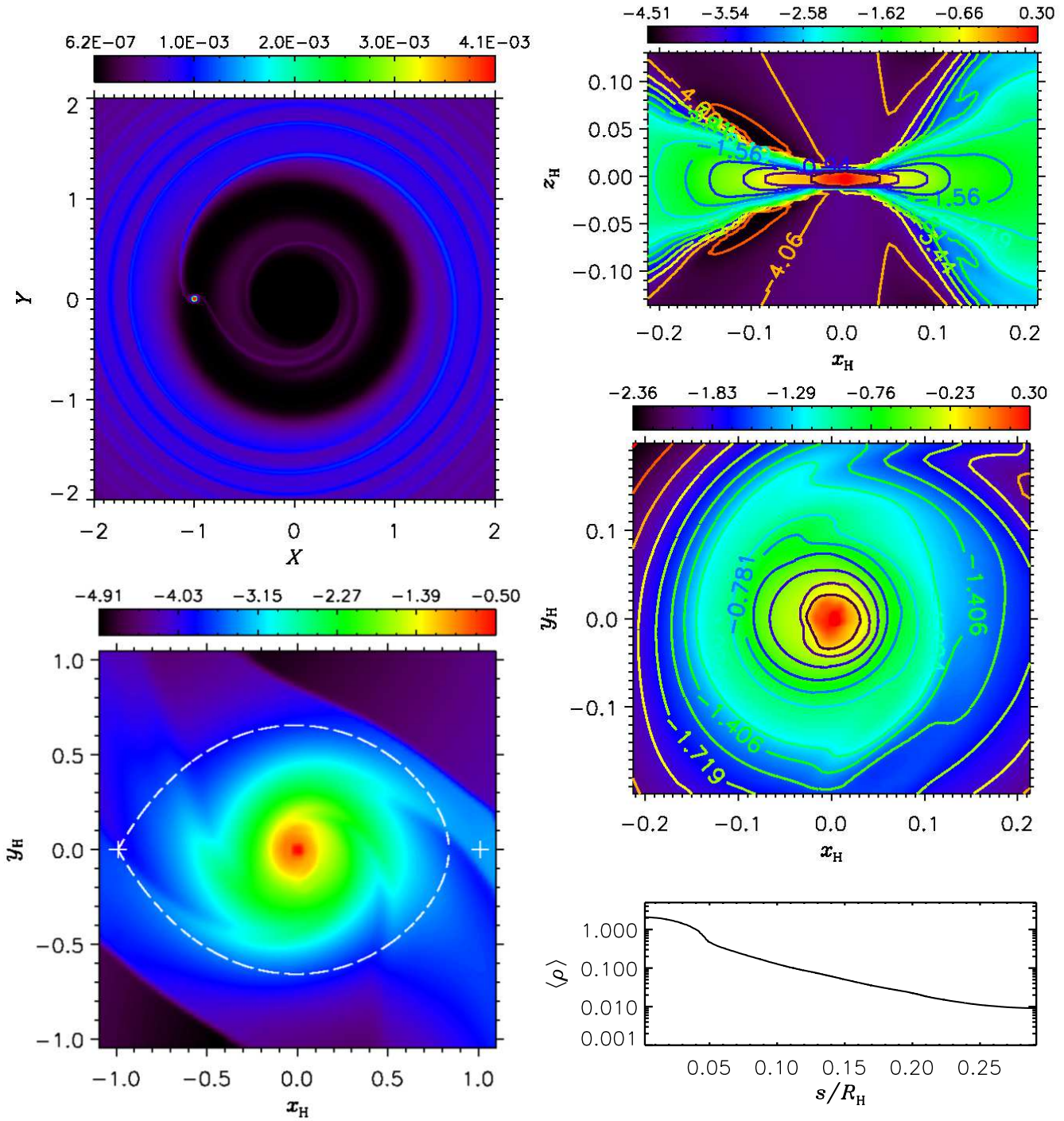


Figure 4: Formation of a circumplanetary disk around a Jupiter-mass planet in 3D. The top panel on the left shows the mass density distribution, ρ , in the circumstellar disk's midplane. The bottom panel on the left as well as the top and center panels on the right show density distributions, in logarithmic scale, within the planet's Roche lobe (the tear-drop shaped region marked by the dashed line). Iso-density contours are also indicated in two panels on the right. The logarithm (base 10) of the azimuthally averaged density, in the disk's midplane, is shown in the bottom panel on the right, where s represents the distance from the planet. The units on the axes are either the planet's orbital radius, r_p (X and Y coordinates), or the Hill radius, R_H (x_H , y_H , and z_H coordinates). The units of ρ are such that 10^{-3} corresponds to $10^{-12} \text{ g cm}^{-3}$.

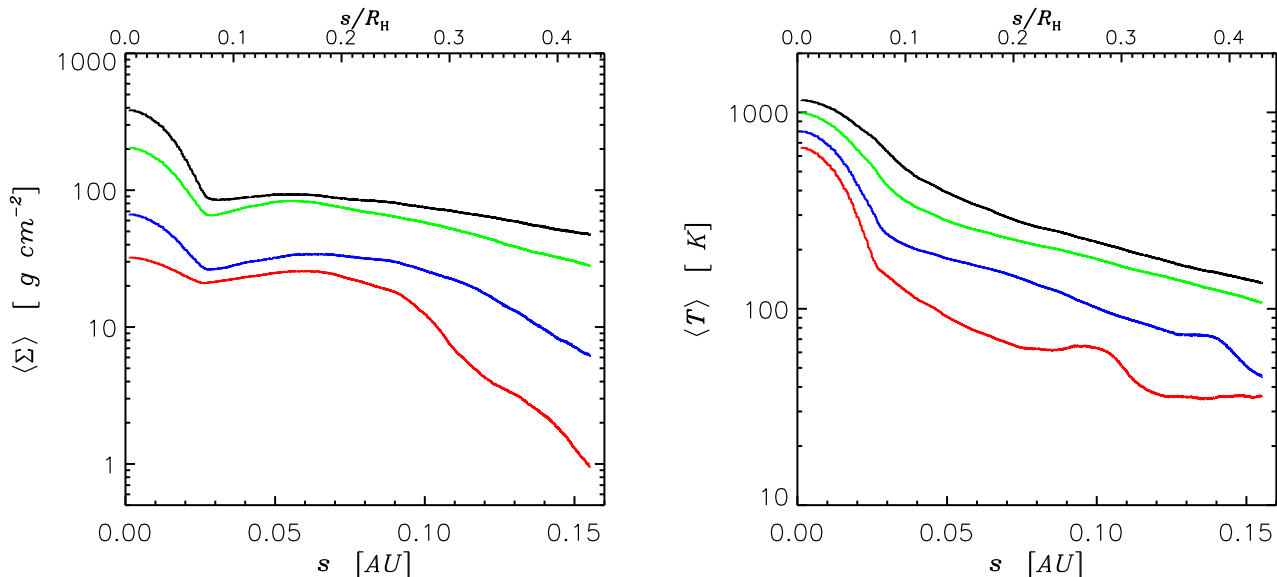


Figure 5: Surface density (left) and temperature (right) of two-dimensional circumjovian disk models with viscous heating and radiative cooling (see text for further details). The quantities represent azimuthal averages around the planet. The models differ in the adopted viscosity prescription. The calculation which produces highest density and temperature (black curve) assumes a constant $\nu = 10^{15} \text{ cm}^2 \text{ s}^{-1}$. The other calculations assume an α -type viscosity, $\nu = \alpha c_s H$ (the same value of α applies to nebula and subnebula) which therefore is space- and time-dependent. For increasing density and temperature, models have $\alpha = 10^{-4}$ (red), 10^{-3} (blue), and 10^{-2} (green), respectively.

(see discussion at the end of Sec. 3.2). The aspect ratio of the circumstellar disk, which is given by the ratio of the disk's semi-thickness (generally denoted by the pressure or nebula scale height H) at the location of the planet to the planet's semi-major axis, is $H/r_p \sim 0.05$. For the disk parameters chosen, ν is comparable to a turbulent viscosity with an α -parameter of 4×10^{-3} at r_p . The top panel on the left illustrates the circumstellar disk and the density gap produced by the planet that exerts gravitational torques on the disk material. The other panels show the mass density, in logarithmic scale, over lengths $\sim R_H$ (left) and $\sim 0.1 R_H$ (right). The bottom panel on the right displays the density in the disk's midplane, azimuthally averaged around the planet, as a function of the distance from the planet, s . The models shown in Fig. 4 can be rescaled by the unperturbed mass density ρ (i.e., that of the circumstellar disk when the planet is not present) at r_p , which is a consequence of the locally isothermal approach. What this means is that the calculated density *structure* in the disk is independent of the value of ρ (i.e., any value of the density gives the same structure). For the value of ρ chosen in Fig. 4, the disk mass within $0.2 R_H$ is $\sim 10^{-4} M_J$.

Alternatively, *D'Angelo et al.* (2003a) present thermo-dynamical models of circumjovian disks in two dimensions. In these calculations, the energy budget of the disk accounts for advection and compressional work, viscous dissipation and local radiative dissipation. Characteristic temperatures and densities in these models depend mainly upon viscosity, opacity tables, and initial mass of the circumstellar disk. In this case, the results are not scalable by the unperturbed mass density, because the opacity depends on the value of ρ chosen.

Figure 5 displays surface density (left) and temperature profiles (right) obtained from calculations with different prescriptions and magnitude of the kinematic viscosity. These models rely on the opacity tables of *Bell and Lin* (1994) and assume that the initial unperturbed surface density, Σ ,

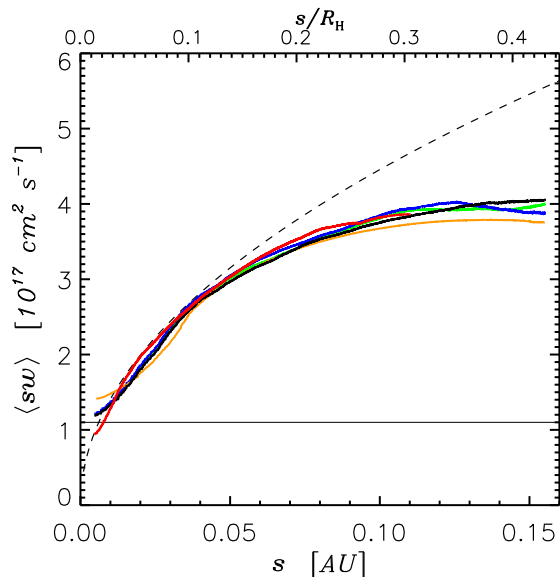


Figure 6: Specific angular momentum of circum-Jovian disk models, in two and three dimensions, azimuthally averaged around the planet. The quantity w is the azimuthal velocity around the planet. Results from models in Figure 4 and Figure 5 are displayed. The orange curve represents the 3D isothermal case. The dashed line represents the Keplerian angular momentum. The horizontal line is the specific angular momentum of the Galilean satellites.

at 5.2 AU is roughly 100 g cm^{-2} . The circumstellar disk contains about 4.8 Jupiter masses within 13 AU of the star. The model with highest density and temperature (black curves) has a constant (in space and time) kinematic viscosity $\nu = 10^{15} \text{ cm}^2 \text{ s}^{-1}$. The other models assume an α -viscosity $\nu = \alpha c_s H$, where the sound speed c_s and the pressure scale height H are a function of space and time while α is a constant. In Fig. 5, for increasing density and temperature, models have $\alpha = 10^{-4}$ (red curves), 10^{-3} (blue curves), and 10^{-2} (green curves), respectively. The value of α applies to both the circumsolar and circumplanetary disks. In the cases shown in the Figure, the amount of mass within about $0.2 R_H$ of the planet is in the range between $\sim 10^{-5} - 10^{-4} M_J$.

The specific angular momentum for three dimensional as well as two dimensional models for a $1 M_J$ mass planet is plotted in Fig. 6. Within $\sim 0.15 R_H$ of the planet, the rotation of the disk follows the rotation curve of a Keplerian disk (dashed curve). The colored curves correspond to the models in Fig. 5, while the orange curve represents the 3D case. It is interesting to note in the latter case that, even though the subnebula temperature is assumed to be constant, the specific angular momentum distribution is consistent with that of the 2D models which are determined by means of calculations that allow for heating and cooling processes. Thus, it appears that for large planetary masses in which a deep gap is present in the circumstellar gas disk, 2D and 3D simulations give comparable results. This is because the gas flowing across such a deep gap into the Roche lobe is coming from much further away (see upper left panel of Fig. 4). Although the flow pattern in 2D and 3D differ, by the time the gas reaches the planet the specific angular momentum delivered with the inflow in both cases is qualitatively similar.

Finally, for comparison, the specific angular momentum of the Galilean satellites is also indicated (solid horizontal line). These simulations confirm our analytical estimate in Sec. 3.2 by indicating that gaps correspond to higher specific angular momentum, and a larger characteristic disk size formed by the inflow, than that of the regular satellites themselves.

3.4. Connecting the Planet, its Disk, and the Satellites

As was pointed out in Sec. 3.2, planetary formation models tend to focus on either the growth of the planet in isolation (Sec. 2), or a protoplanet of fixed mass embedded in a circumstellar disk in the presence of a well formed gap (Sec. 3.3). As a result, our understanding of the formation

of the circumjovian gas disk remains incomplete, as no simulations have yet been done that model disk formation from just after the giant planet’s envelope contraction to the time at which inflow from the circumsolar disk ceases.

During the period over which disk formation occurs, the characteristic disk size may be roughly estimated by a balance between gravitational and centrifugal forces (Sec. 3.2). Because the proto-planet likely accretes most of its gas mass after envelope collapse, a significant fraction of this gas may end up in the circumjovian gas disk leading to an initially massive subnebula. A legitimate concern that arises from this scenario is why is it that Jupiter is not rotating near break-up velocity? The origin of Jupiter’s current spin angular momentum remains poorly understood. A massive circumplanetary disk may be a requirement for despinning the planet (see e.g., *Korycansky et al.*, 1991; *Takata and Stevenson*, 1996). The question of Jupiter’s spin thus represents a key piece of the Jovian system puzzle that is in need of further investigation.

A compact massive disk will have important implications for satellite formation models. However, the characterization of this disk component will require the marriage of isolated growth models and embedded planet simulations, a milestone that is just beginning to be explored. Indeed, recent simulations of gas accretion onto a low-mass protoplanet (i.e., a deep gap is not present) embedded in a circumstellar disk indicate that gas may not be bound to the planet outside of $\sim 0.25 R_H$ (*Hubickyj et al.*, 2007). Preliminary measurements of the specific angular momentum contained within the bound region for different pre-gap-opening protoplanet masses are consistent with Eq. 5 (yielding $\ell \sim \Omega R_H^2/4$), despite this equation being based on unrealistic assumptions.

Recently, *Machida et al.* (2008) use 3D hydrodynamical simulations to model the angular momentum accretion into the giant planet Hill sphere when a partially depleted gap is present. These authors find for a range of planetary masses that a significant fraction of the total angular momentum may contribute to the formation of a compact circumplanetary disk. An important conclusion that may be drawn from the results of *Machida et al.* is that a circumplanetary disk formed when a partial gap is present is compact due to the lower specific angular momentum of the inflow. However, these results are inapplicable for masses comparable to $1 M_J$. This is because for planets this massive, a deep, well-formed gap would be present.

Finally, for large planetary masses in the presence of a deep gap, the circumplanetary disk size is qualitatively insensitive to the inflow rate, or whether the flow is treated in 2D or 3D. However, 3D simulations are required early on in the accretion of the protoplanet when a deep gap is not present. We can understand this by noting that material in the nebula midplane whose semimajor axis is close to the planet ($\lesssim R_H$) actually does not accrete onto the planet, but instead undergoes horseshoe orbits (e.g., *Lubow et al.*, 1999; *Tanigawa and Watanabe*, 2002). Three-dimensional flows are then necessary to allow for low angular momentum gas from radial distances $\lesssim R_H$ and away from the midplane to be accreted directly onto the planet or into a compact disk (*Bate et al.*, 2003; *D’Angelo et al.*, 2003a). Moreover, *D’Angelo et al.* (2003b) point out that because of the flow circulation away from the disk midplane, less angular momentum is carried inside the Roche lobe by the midplane flow, so that in general 3D simulations are required in order to properly account for the angular momentum.

What does this all mean for the formation of the Galilean satellites which lie in a quite compact region close to the planet? When a well-formed gap is present, the characteristic circumjovian disk size formed by the inflow is $> 0.1 R_H$, or $> 70 R_J$ (by comparison Ganymede is located at $\sim 15 R_J$). From Fig. 6, it can be seen that the specific angular momentum of the inflow is about a factor of 3 – 4 larger than that of the Galilean satellites ($\sim 1.1 \times 10^{17} \text{ cm}^2 \text{ s}^{-1}$), which means that the gas will achieve centrifugal balance at a radial location of $\sim 200 R_J$. While this disk is compact compared to R_H , it is extended in terms of the locations of the Galilean satellites, and possibly

linked to the location of the irregulars (the innermost ones of which lie near $\sim 150 R_J$). Thus, these results indicate that the inflow through a gap in the circumsolar disk results in an extended circumplanetary disk of characteristic size $\sim 70 - 200 R_J$, implying a mismatch between the size of the circumplanetary disk formed by gas inflow through the giant planet’s gap and the compact region where the regular satellites are found.

This mismatch has important consequences for satellite formation. Taken at face value, it may mean one of two things: (i) the solid material coupled to the gas coming through the gap did not provide the bulk of the material that formed the regular satellites – planetesimals that were not coupled to the gas provided this source instead (see Sec. 4.2); or (ii) the regular satellites migrated distances considerably larger than their current locations. The first option would effectively preclude gas inflow through the gap as the source of solids for regular satellite formation. The second option would make questionable any model that explains the Galilean satellite compositional gradient with subnebula “snow line” arguments; that is, all satellites would presumably start out far from the planet and outside the snowline, and receive their full complement of ices.

These options assume that after gap-opening the disk becomes cool enough, and thus the inflow is weak enough, that icy objects can form. Prior to gap-opening, the inflow is likely to be fast so that the circumplanetary disk would be too hot for the concurrent formation of ice-rich satellites like Callisto and Ganymede. Therefore, it is not possible to form a compact disk concurrently with the accretion of ice-rich, close-in satellites, indicating that satellite formation doesn’t begin until the gas inflow wanes and turbulence decays, or the subnebula gas disk has dissipated.

4. CONDITIONS FOR SATELLITE FORMATION

In the core nucleated accretion model, Jupiter’s formation is viewed to occur in three stages (Sec. 2): *nebular*, *transition*, and *isolation*. Within the sequence of events that these stages characterize, we may now identify the formation of the circumjovian gas disk as occurring during the transition stage of Jupiter’s accretion. The formation of the subnebula should be viewed as a drawn out process that begins post envelope contraction and ends when Jupiter is isolated from the solar nebula. In order to complete this picture, we need to describe when and how satellite formation fits into this sequence. The possible accretion environments in which the satellites may form depend on the planet-disk evolutionary track that is followed, so it is important to summarize the sequence of events that are viewed to occur for a plausible Jupiter accretion scenario (i.e., a final mass of $1 M_J$), prior to satellite formation:

1. During the *nebular* stage of Jupiter’s growth, most of the solids reside in large planetesimals, some of which may dissolve in the growing envelope during the latter part of this stage. Most of the high-Z mass delivery takes place before the “cross-over” time, when the mass of the gaseous envelope grows larger than the core. This stage of growth may be followed by a *dilution* as the solids accretion rate drops off and the gas accretion rate accelerates.
2. As the envelope becomes massive enough, it eventually contracts and accretes gas (of low specific angular momentum) from the circumsolar disk hydrodynamically (*transition* stage). Contraction down to a few planetary radii happens quickly relative to the runaway gas accretion timescale, and is expected to occur when the protoplanet is still a relatively small fraction of its final mass. Because a significant fraction of the gas in the envelope has too much rotational angular momentum, it collapses onto a relatively compact disk. The contraction of the envelope thus marks the initial stage of subnebula formation.

3. After envelope collapse, the protoplanet’s mass is still too small for it to clear a significant gap in the surrounding solar nebula, so most of the gas flowing into the Roche lobe continues to originate from regions in the vicinity of the protoplanet ($\lesssim R_H$). This gas accretes onto both the planet and a rotationally supported compact disk. Because the protoplanet still must accrete the bulk of its mass at this stage, a substantial amount of gas may end up in the circumjovian disk. As the protoplanet becomes more massive, it more readily perturbs the nebula gas and depletes the gas in its vicinity.
4. The truncation of the solar nebula gas disk (due to the opening of a deep well-formed gap) likely occurs towards the tail end of the runaway gas accretion phase when Jupiter is approaching its final mass. Saturn, if present and nearby, also likely delays the opening of a deep gap. As the proto-Jupiter begins to truncate the disk, nebula gas continues to flow through the Lagrange points (see Fig 4). This leads to the formation of an extended disk because gas parcels now come from considerably farther away in semi-major axis than R_H . Meanwhile, planetesimals in Jupiter’s feeding zone undergo an intense period of collisional grinding leading to a fragmented population (Sec 4.2). Continued solids enhancement of the entire circumjovian disk occurs due to ablation of disk-crossing planetesimal fragments (see Fig. 7).

What happens next largely depends on the assumed level and persistence of turbulence in both the circumsolar and circumplanetary nebulae.

4.1. Turbulence and its Implications for Satellite Accretion

For disks to accrete onto the central object, angular momentum must be transported outwards. In the case of disks around young stellar objects (YSOs), magneto-hydrodynamic (MHD) and self-gravitating mechanisms have been investigated in some detail (e.g., *Gammie and Johnson*, 2005). The self-gravitating mechanism, which is presumably stronger, eventually turns itself off as the gas disk dissipates, at which point MHD may gain relevance. Differentially rotating disks are known to be subject to a local instability referred to as a magneto-rotational instability, or MRI (*Balbus and Hawley*, 1991). While these disks may be sufficiently magnetized, significant portions of the disk (specifically the planet formation regions) may have ionization that is too low for MRI to be effective, creating a “dead zone” (*Gammie*, 1996; *Turner et al.*, 2007), or region of inactivity.

On the other hand, in the absence of an MHD mechanism, one would have to resort to a purely hydrodynamic mechanism. However, it is well known that hydrodynamic Keplerian disks are stable to linear perturbations (e.g., *Ryu and Goodman*, 1992; *Balbus et al.*, 1996). Possible sources of turbulence such as convection (*Lin and Papaloizou*, 1980) and baroclinic effects (*Li et al.*, 2000; *Klahr and Bodenheimer*, 2003) may provide inadequate, decaying transport in 3D disks (*Barranco and Marcus*, 2005; *Shen et al.*, 2006), subside as the disk becomes optically thin, and may fail to apply to isothermal portions of the disk. A number of analytical studies have suggested transient growth mechanisms for purely hydrodynamic turbulence that would lead to the excitation of non-linear behavior (*Chagelishvili et al.*, 2003; *Umurhan and Regev*, 2004; *Afshordi et al.*, 2005). However, numerical simulations (*Hawley et al.*, 1999; *Shen et al.*, 2006) and laboratory experiments (*Ji et al.*, 2006) cast doubt on the ability of purely hydrodynamic turbulence to transport angular momentum efficiently in Keplerian disks even for high Reynolds number (*Lesur and Longaretti*, 2005). Although the evidence that Keplerian disks are laminar is not conclusive because the Reynolds numbers in disks are much larger than those accessible to computers or experiments, it is fair to say that what makes disks around YSOs accrete remains an open problem.

While there is a consensus that both the nebula and the subnebula undergo turbulent early phases, we are presently lacking a mechanism that can sustain turbulence in a dense, mostly isothermal subnebula (*Mosqueira and Estrada*, 2003a,b). In order to sidestep this problem, one is then forced to postulate a low density gas disk (*Estrada and Mosqueira*, 2006), and invoke MRI turbulence to sustain turbulence in such a disk. But here again the likely presence of dust complicates the situation even in the low density case. Hence, a sufficiently general mechanism for sustaining turbulence in poorly ionized disks has yet to be found, suggesting that alternative mechanisms of disk removal need to be explored. In particular, the role that the planets and satellites themselves play in driving disk evolution has only begun to be explored (*Goodman and Rafikov*, 2001; *Mosqueira and Estrada*, 2003b; *Sari and Goldreich*, 2004).

4.2. Methods of Solids Delivery

There are several ways in which solids can be delivered to the circumjovian disk. Although all of these mechanisms likely played a role in satellite formation, it should be emphasized that at the time of giant planet formation, most of the available mass of solids are in planetesimals in sizes $\gtrsim 1$ km (*Wetherill and Stewart*, 1993; *Weidenschilling*, 1997; *Kenyon and Luu*, 1999; *Charnoz and Morbidelli*, 2003). In the Jupiter-Saturn region the collisional timescale for kilometer-sized objects is similar to the ejection timescale ($\sim 10^5$ years, *Goldreich et al.*, 2004), so that a significant fraction of the mass of solids are fragmented into objects smaller than ~ 1 km (*Stern and Weissman*, 2001; *Charnoz and Morbidelli*, 2003). Sufficiently small planetesimals (~ 1 m) are protected from further collisional erosion by gas-drag and by collisional eccentricity and inclination damping. Given that fragmentation likely plays a significant role in the continued evolution of the heliocentric planetesimal population following the formation of Jupiter (*Stern and Weissman*, 2001; *Charnoz and Morbidelli*, 2003), the 1 m – 1 km size range of planetesimals likely plays a key role in satellite formation.

I. Break-up and dissolution of planetesimals in the extended envelope. Because the giant planet envelope probably filled a fair fraction of its Roche lobe during a significant fraction of its gas accretion phase, its cross section would have been greatly increased (*Bodenheimer and Pollack*, 1986; *Pollack et al.*, 1996), so that early arriving planetesimals could break up and/or dissolve in the envelope, enhancing its metallicity. In the earliest stages of growth when the envelope mass is low, most planetesimals will likely reach the core intact. As the gaseous envelope becomes more massive, planetesimals begin to deposit significant amounts of their mass in the distended envelope (e.g., *Podolak et al.*, 1988). Some dust and debris deposited during the extended envelope and relatively rapid envelope collapse phases would have been left behind in any subsequent subnebula “seed” created as a result of the planet’s contraction (especially if the planet were rotating rapidly).

II. Ablation of planetesimals through the circumjovian gas disk. Depending on the gas surface density of the subnebula, disk crossers ($\gtrsim 1$ m) can either ablate, melt, vaporize or be captured as they pass through the disk. A significant amount of material could be deposited in the form of planetesimal fragments down to dust and debris. The total mass delivered depends on the surface density of solids in the solar nebula, as well as the deposition efficiency, but it may be possible to deliver several times the mass of the Galilean satellites, much of which could have been lost due to the inefficiencies of satellite accretion.

III. Collisional capture of planetesimals. Once the planetesimal population has been perturbed into planet crossing orbits (*Gladman and Duncan*, 1990), both gravitational and inelastic collisions between planetesimals within Jupiter’s Hill sphere occur. If inelastic collisions occur between planetesimals of similar size, the loss of kinetic energy through their collision can lead to capture, and eventually the formation of a circumplanetary accretion disk. Gravitational collisions between

planetesimals, owing to their larger effective gravitational cross-sections, will lead to mass capture.

IV. Dust coupled to the gas inflow through the gap. Essentially all numerical models of giant planet formation indicate that there is flow of gas through the gap, with the strength of the flow dependent on the assumed value of the solar nebula turbulence (e.g., *Artymowicz and Lubow*, 1996; *Lubow et al.*, 1999; *Bryden et al.*, 2000; *Bate et al.*, 2003; *D’Angelo et al.*, 2003b). None of these studies incorporated dust in their simulations; however, there are numerous arguments one may pose as to why dust inflow cannot be the dominant source of material (for more discussion, see *Mosqueira and Estrada*, 2003a; *Estrada and Mosqueira*, 2006). First, little mass remains in dust at the time of planet formation (*Mizuno et al.*, 1978; *Weidenschilling*, 1997; *Charnoz and Morbidelli*, 2003). Second, as was demonstrated in Sec. 3.3, the specific angular momentum of the inflow deposits a significant fraction of the mass (along with the gas) at large distances in the circumplanetary disk possibly leading to the formation of satellites far from the planet where they are not observed. Third, the edges of gaps opened by giant planets act as powerful filters restricting the size and amount of dust that can be delivered this way (*Paardekooper and Mellema*, 2006; *Rice et al.*, 2006) with entrained particle sizes orders of magnitude smaller than the local decoupling size (recall, ~ 1 m at Jupiter). Fourth, what is relevant is the dust content of the inflowing gas which may be substantially decreased with respect to solar nebula gas; i.e., embedded planet simulations in 3D show that the gas inflow comes from lower density regions (e.g., see Fig. 4) above and below the midplane (e.g., *Bate et al.*, 2003; *D’Angelo et al.*, 2003b), with the typical maximum flow velocity occurring at a pressure scale height. This would further restrict particle sizes entrained in the gas inflow.

4.3. Gas-rich Environment

In Section 3, we discussed the formation of a massive circumplanetary disk. Traditionally, the approach has been to calculate (akin to the MMSN) a minimum mass model for the circumjovian disk. In such a model, the total disk mass (gas + solids) is set by spreading the re-constituted mass (accounting for lost volatiles) of the Galilean satellites over the disk and adding enough gas to make the subnebula solar in composition (typically a factor of ~ 100 , e.g., *Pollack et al.*, 1994). The total mass of the circumplanetary disk that results from this approach described above is $\sim 10^{-2} M_J$ (note that the disk-to-primary mass ratio for Jupiter is similar to Sun). Moreover, if one calculates the total angular momentum contained within this gaseous disk, one finds it is (perhaps by no coincidence) comparable to the spin angular momentum of Jupiter (*Stevenson et al.*, 1986; see Table 3, *Mosqueira and Estrada*, 2003a). Thus the notion of an equipartition of angular momentum between planet and disk is consistent with a massive subnebula.

4.3.1. Decaying Turbulence Satellite Formation Scenario. As long as gas inflow through the gap continues, the circumplanetary disk should remain turbulent (driven by the inflow itself) and continue to viscously evolve until the gas inflow from the circumsolar disk wanes in a timescale of $< 10^5$ years or shorter in a weakly turbulent solar nebula (*Bryden et al.*, 1999, 2000; *Mosqueira and Estrada*, 2006; *Morbidelli and Crida*, 2007). As the subnebula evolves, the gas surface density lowers. Once the gas inflow ceases and disk evolution stalls, a different driving mechanism is needed to facilitate further disk evolution.

This circumplanetary disk environment in which the regular satellites form has been dubbed the Solids Enhanced Minimum Mass (SEMM) disk (*Mosqueira and Estrada*, 2003a,b), because satellite formation occurs once sufficient *gas* has been removed from an initially massive subnebula and turbulence in the circumplanetary disk subsides. The SEMM disk is enhanced in solids because there are processes by which the disk ends up with a gas-to-solids ratio less than solar. In particular, preferential removal of gas (e.g., *Takeuchi and Lin*, 2002) during the inflow-driven subnebula

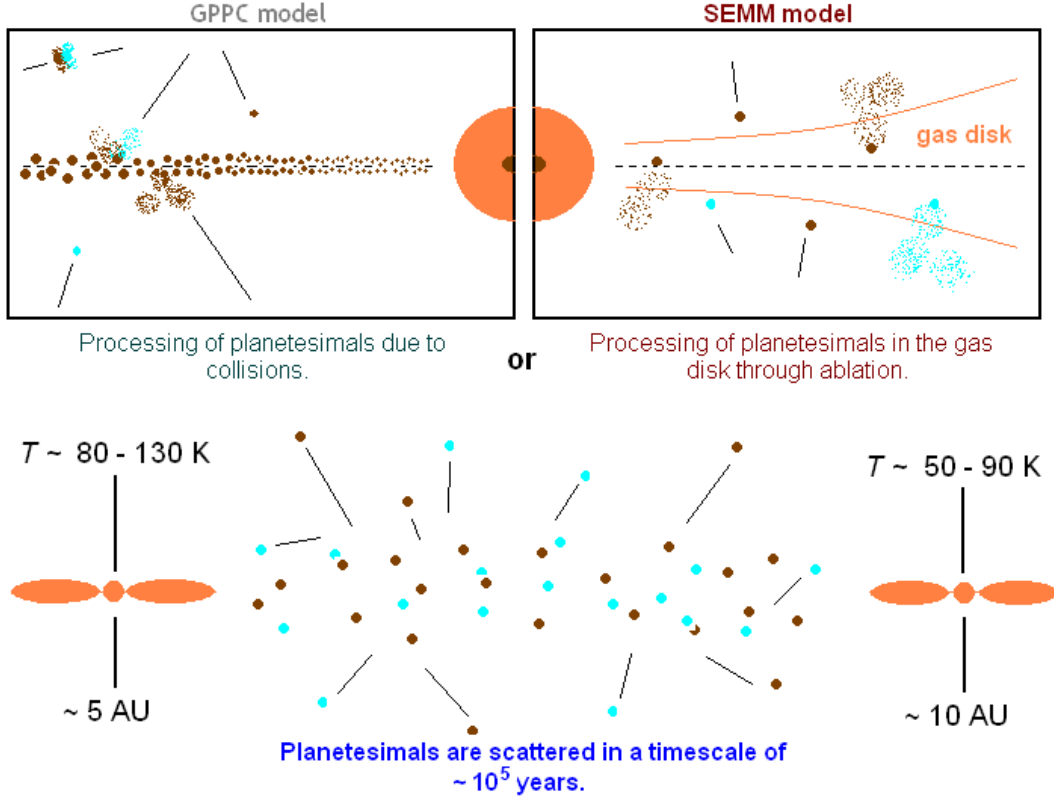


Figure 7: Vignette of the dominant planetesimal delivery mechanisms (Sec. 4.2) for the two satellite formation environments discussed. In the left window is the gas-poor planetesimal capture (GPPC) model for the circumjovian disk in which processing of planetesimals occurs through planetesimal-planetesimal, and planetesimal-satellitesimal collisions. In the right window is the solids-enhanced minimum mass (SEMM) model for the circumjovian disk in which processing of heliocentric planetesimals occurs through their ablation as they pass through the Jovian subnebula. The different scenarios have implications for the compositional evolution of the Galilean satellites. In either case, it is expected that the planetesimal population in the feeding zone of Jupiter (or between Jupiter and Saturn, if Saturn is present) will mostly be scattered away in $\sim 10^5$ years. Much of this material may have a chance to end up in the circumplanetary disk through collisional capture and/or through direct passage across the disk plane prior to being scattered.

evolution phase may lead to enhancement of solids in the circumplanetary disk, while continued further enhancement occurs through the ablation of heliocentric planetesimal fragments that cross the circumplanetary disk plane. Such a disk may then be enhanced in solids by a factor of $\sim 3 - 4$ consistent with the solids enhancement observed in the Jovian atmosphere. We stress that the properties of a SEMM model are distinct from those of a minimum mass model in terms of disk cooling, and satellite formation and migration timescales.

4.3.2. Satellite Growth in the Circumjovian Disk. The growth of satellitesimals and embryos in the circumplanetary disk is assumed to be controlled first by sweepup of dust and rubble (e.g., *Cuzzi et al.*, 1993; *Weidenschilling*, 1997). As the inflow from the circumsolar disk wanes and turbulence decays, the inner more massive region becomes weakly turbulent (while the outer extended disk becomes isothermal and quiescent). Once this occurs, dust coagulation and settling is assumed to proceed rapidly given that dynamical times are $\gtrsim 10^3$ times faster in the inner disk of Jupiter than

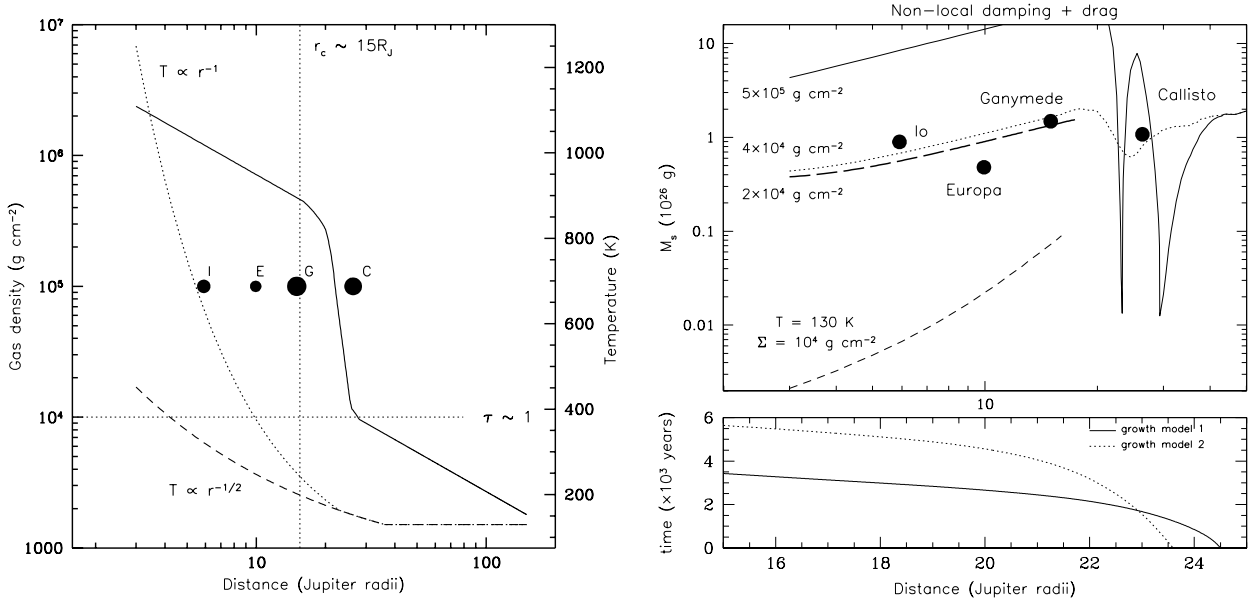


Figure 8: Left: Idealization of the initial Σ and assumed photospheric T profiles for the circumjovian subnebula. The re-constituted mass of Io, Europa, and Ganymede determine the mass of the optically thick inner disk, while the mass of Callisto is spread out over the optically thin outer disk. Ganymede lies just inside the centrifugal radius r_c , while Callisto lies outside a transition region that separates the inner and outer disks. The transition region between the inner and outer disks is assumed (see text). The temperature is set to agree with the compositional constraints of the Galilean satellites (e.g., *Lunine and Stevenson, 1982; Mosqueira and Estrada, 2003a,b*), which implies a Jovian luminosity of $\sim 10^{-5} L_\odot$, for a planetary radius of $\sim 1.5 - 2 R_J$ consistent with planet formation models (*Hubickyj et al., 2005; Fig. 1a*). Upper left: Critical mass at which migration stalls as a function of Jupiter radii for various Σ -profiles using both vertically thermally stratified (solid and dotted curves), and vertically isothermal models (bold dashed curve). Gas drag is included. The solid curve corresponds to the minimum mass model, while the dotted and dashed curves correspond to the SEMM model. The short-dashed curve is a constant Σ and T model. Lower right: Migration and growth models for proto-Ganymede. The full sized Ganymede is evolved backward in time from the location where it opens a gap to the point where it reaches embryo size (~ 1000 km) for a SEMM disk. Two models for growth are used. Solid curve: linear growth model. Dotted curve: growth rate proportional to the disk surface density. Growth is consistent with the limited migration of Ganymede. See *Mosqueira and Estrada, 2003b* for detailed descriptions.

in the local solar nebula.

Once a significant fraction of the solids in the disk have aggregated into objects large enough to decouple from the gas (radii $R \gtrsim 10 - 100$ m) and settle to the disk midplane, they drift inward due to gas drag at different rates, leading to further “drift-augmented” accretion. In the weak turbulence regime, the ratio of the sweepup time (which assumes most of mass of the disk is initially in small particles entrained in the gas) to gas drag is

$$\frac{\tau_{\text{sweep}}}{\tau_{\text{gas}}} \approx \frac{4\rho_s R}{3\bar{\rho}_p \Delta v} / \frac{4\rho_s R v_K}{3C_D \rho (\Delta v)^2} \sim C_D \eta \frac{\rho}{\bar{\rho}_p} < 1, \quad (7)$$

quite generally in the inner (and outer) disk. Here, $\bar{\rho}_p$ is the average solids density in the midplane,

ρ_s is the satellitesimal density, C_D the gas drag coefficient, and $\eta = \Delta v/v_K$ (e.g., $\eta \sim 10^{-2}$ at Ganymede) measures the difference between v_K and the pressure supported gas velocity. This is a significant result because it means that satellite formation is always favorable (even for the case of the more massive minimum mass subnebula, $\rho/\bar{\rho}_p \lesssim 100$ because of settling). Equation (7) further implies that it is possible to form satellites/embryos of any size < 1000 km (such that gas drag dominates their inward migration) at any radial location in the inner disk. Eventually as the reservoir of dust and rubble is depleted, sweepup is less efficient, and growth of the embryo begins to be controlled by gas drag drift-augmented accretion of satellitesimals and smaller embryos.

As the satellite embryo continues to grow, accretion becomes more efficient because the embryo becomes an effective barrier (due to high impact probabilities; *Kary et al.*, 1993) for inwardly drifting material. A natural by-product of becoming an effective barrier is the choking off of the supply of material to its nearest inner neighbor, thus potentially limiting its final size. Once embryos become effective barriers, the timescale to complete their formation is determined by the inward drift time of the characteristic size (and distance from which they migrate) of satellitesimals (or embryos) it accretes. In this picture Ganymede forms in $\sim 10^3 - 10^4$ years.

In contrast, although growth of satellitesimals and embryos in the outer, lower density portions of the disk is qualitatively similar (with some subtle differences, see *Mosqueira and Estrada*, 2003a), Callisto’s formation time is determined by the time it takes to clear the solids from the outer circumplanetary disk. One significant difference that arises is that embryos that form in the outer disk become isolated from one another as they drift inwards. By isolation, it is meant that collisions between migrating embryos steeply drop off, and occur at the escape velocity of embryos which may lead to growth or fragmentation (e.g., *Agnor and Asphaug*, 2004). As embryos approach proto-Callisto (which eventually also becomes an effective barrier), they begin to be perturbed into crossing orbits, and collisions would occur at the proto-Callisto’s escape velocity, likely leading to fragmentation of the inwardling drifting embryos into smaller bodies (*Mosqueira and Estrada*, 2003a; See Sec. 4.5). Thus Callisto’s formation timescale is dictated by the time it takes this “slow stream” of inward drifting cold embryos to migrate to its location, or roughly $\lesssim 10^6$ years for the outer disk gas surface density shown in Fig. 8.

It is important to note that while satellite embryos form quickly, the SEMM model has full-sized satellites forming on a longer timescale. This is because, unlike traditional minimum mass models, the SEMM model is not a local growth model; i.e., a full-sized satellite formation timescale is controlled by the timescale over which the feeding zone of the embryo is replenished by other embryos or satellitesimals. Thus, the mass of the satellites is spread out over the entire disk, and full-sized satellites must accrete material from well outside their feeding zones. In fact, most of the present day satellite disk is empty, presumably due to gas drag clearing of satellitesimals.

4.3.3. Satellite Survival in a Gas-rich Disk. A gas-rich disk promotes accretion of satellites; however, such a disk can also lead to orbital decay or even loss of satellites on timescales much faster than it would take the circumplanetary gas disk to dissipate naturally. On the one end, gas drag (Sec. 2.1) leads to a head-wind that causes smaller objects to drag inwards towards the primary (e.g., *Weidenschilling*, 1988), and is the primary mechanism for drift-augmented accretion. On the other end, because much larger objects can interact gravitationally with a gaseous disk at Lindblad resonances (see *Goldreich and Tremaine*, 1979), protosatellites must contend with gas tidal torques that may lead to catastrophically fast migration rates (via “type I” migration; *Ward*, 1997). The direction of migration is generally inward towards the primary.

As a satellite grows in size, its migration speed increases (the torque is proportional to the mass squared), but at the same time so does the satellite’s perturbation of the gas disk. If the accretion rate of the satellite is faster than the type I migration rate, *and* if the satellite can achieve

a certain critical mass, asymmetries in the torque contributions from inside and outside the orbit of the satellite can balance, and the satellite slows and stalls relative to the gas (Ward, 1997; Rafikov, 2002b). Once stalled, the satellite may begin to open and clear a gap in the subnebula. Another consequence of the satellite’s tidal interaction with the disk (and subsequent angular momentum transfer) is that the migrating satellite can actually drive radial evolution of the disk (e.g., Sari and Goldreich, 2004) by producing a local viscosity leading to gas clearing (Goodman and Rafikov, 2001). However, the physics of disk-satellite interactions is complex. We simply note that models which employ strong, persistent turbulence do not include tidal torque migration, because the gas disk evolves too quickly (e.g., Canup and Ward, 2002; Alibert et al., 2005a; Estrada and Mosqueira, 2006) for tidal migration to be important.

The stalling mechanism described above offers an attractive alternative for generating the viscosity necessary to drive disk evolution further once turbulence decays. Motivated by this, Mosqueira and Estrada (2003b) explored static models of the Jovian subnebula and determined the conditions under which the largest satellites may stall, open gaps, and survive under gas-rich conditions for specific models of angular momentum dissipation (see Mosqueira and Estrada, 2003b for details). Figure 8 (upper right panel) shows results of these calculations. First, their results indicate that a “minimum mass disk” (solid curve) is likely too massive to allow for the survival of any of the inner disk Galilean satellites, and that a significant decrease in the gas surface density is required for stalling to be possible (dotted and bold long-dashed curves, SEMM disk). Second, the critical mass for which a satellite may stall its migration increases with distance from Jupiter which allows a satellite to drift in until it finds an equilibrium position, so long as it is sufficiently massive to stall somewhere in the disk. The largest masses tend to be located near the centrifugal radius. Finally, due to the strong gradient in the disk temperature (assumed to be controlled by Jupiter’s luminosity, see Fig. 1), the slope of the curves in Fig. 8 are shallow limiting the range of masses that may stall with mass ratios of satellite to planet of $\mu \sim 10^{-4}$. Additionally, the density waves launched by objects of this size shock-dissipate in a length scale smaller than their semimajor axis (Goodman and Rafikov, 2001).

It must be mentioned that there are a number of assumptions involved in the results described above. The initial gas surface density has been obtained by placing Callisto in the outer disk, and Ganymede, Europa, and Io in the inner disk, separated by an assumed transition between the outer and the inner disks. However, there are presently no detailed simulations of the formation of such a disk. Furthermore, the temperature structure of the disk is heuristic. Nevertheless, we stress that the overall survival mechanism need not be dependent on the specifics of the model. For instance, Callisto may stall because its migration is halted by the change in the surface density due to the presence of Ganymede. Alternatively, satellites may open gaps collectively. This latter option would be particularly relevant if satellite-disk interactions can result in eccentricity growth which would result in spatially extended gap formation. Another process to consider is photoevaporation, which may take place in a timescale comparable to that of the formation and migration of Callisto (and Iapetus for Saturn). The key point here is that the largest satellites of each satellite system and not turbulence may be responsible for giant planet satellite survival.

Finally, it is useful to evaluate whether migration times are consistent with the growth timescales of the Galilean satellites. This is useful because it also allows a way of estimating how far the satellite may have migrated. By associating the current locations of the satellites with their stalling location (Fig. 8, upper right panel), Mosqueira and Estrada (2003b) integrated the migration of the full-sized Ganymede back in time to embryo size using different growth models (Fig. 8, lower right panel). The results imply that SEMM disks are consistent with the limited migration of at least Ganymede, so that Ganymede formed close to the location of the centrifugal radius, r_c .

4.4. Gas-poor Environment

In the gas-poor scenario sustained turbulence (possibly hydrodynamic turbulence) or some other mechanism removes the gaseous circumplanetary disk relatively quickly compared to the accretion timescale of the satellites (which is tied to the timescale for clearing heliocentric planetesimals from the giant planet’s feeding zone). As a result, satellite formation is somewhat akin to the formation of the terrestrial planets, which also treats the gas surface density as being low but unspecified.

Because the disk is assumed to be gas depleted, the gas-poor environment does not face the survival issues associated with the presence of significant amounts of gas; yet, one may still use the remnant circumplanetary gas disk to circularize orbits, or to clear the disk of collisional debris. However, the way in which the solid material that makes up the satellites is delivered to the circumplanetary disk must differ significantly from the gas-rich case. This is because much of the dust and debris that was entrained in the subnebula gas prior to its removal is lost due to the rapid viscous evolution of the disk, while any gas inflow through the giant planet gap is expected to have low dust content. Thus, this scenario relies on the formation of an accretion disk resulting from the capture into circumplanetary orbit of heliocentric planetesimals undergoing inelastic (*Safronov et al.*, 1986; *Estrada and Mosqueira*, 2006; *Sari and Goldreich*, 2006), or gravitational (*Goldreich et al.*, 2002; *Agnor and Hamilton*, 2006) collisions within the Jovian Hill sphere (see Sec. 4.2). Furthermore, it also means that, unlike the environment described in the previous section in which gas dynamics dictates the angular momentum budget of the satellites, the angular momentum of the satellite system is largely determined by circumsolar planetesimal dynamics.

4.4.1. The Circumplanetary Swarm. The idea that the regular satellites could form out of a collisionally-captured, gravitationally-bound swarm of circumplanetary satellitesimals has been suggested and explored in a number of classic publications (*Schmidt*, 1957; *Safronov and Ruskol*, 1977; *Ruskol*, 1981, 1982; *Safronov et al.*, 1986). However, it has only been in recent time that a specific scenario for satellite formation has been advanced (the gas-poor planetesimal capture, or GPPC model; *Estrada and Mosqueira*, 2006). More recently, collisional capture mechanisms have been explored in terms of general accretion (*Sari and Goldreich*, 2006), and applied to the formation of Kuiper Belt binaries (*Schlichting and Sari*, 2007).

The GPPC formation scenario is separated into two stages: an early stage in which the circumplanetary disk is initially formed, and a late stage in which a quasi-steady state accretion disk is in place around the giant planet. In the early stage, the idea is that inelastic and gravitational collisions within the Hill sphere of the giant planet lead to the possibility of capture by the planet’s gravitational field. Planetesimal capture leads to the creation of a protosatellite “swarm” of both retrograde and prograde satellitesimals extending out as far as circumplanetary orbits are stable, $\sim R_H/2$. At the present time, the complicated process of circumplanetary swarm generation remains to be modeled.

Estrada and Mosqueira (2006) have modeled the late stage of satellite formation in a gas-poor environment in which a circumplanetary accretion disk is assumed to be already present, and that inelastic collisions between incoming planetesimals with *larger* satellitesimals within the accretion disk is the more efficient mass capture mechanism. Planetesimal-satellitesimal collisions can lead to the capture of solids if the incoming planetesimal encounters a mass comparable to, or larger than itself (*Safronov et al.*, 1986). This may be a physical collision with a larger satellitesimal, or a number of smaller satellitesimals.

Because the disk has such a large surface area, the total mass of planetesimals that can pass through such a disk may be substantial. A reasonable estimate of the amount of mass in planetesimals in Jupiter’s feeding zone is $\sim 10 M_\oplus \sim 10^{29}$ g. These planetesimals will cross the circumplan-

etary disk many times before being scattered away by Jupiter, and thus may be subject to capture. The amount of mass captured, however, will depend on the size distribution, and total mass of satellitesimals in the accretion disk, as well as the timescale over which heliocentric planetesimals are fed into the system. However, not all of the mass delivered to the circumplanetary disk will be accreted by the regular satellites. Bound objects may be dislodged by passing planetesimals, or during close encounters between the giant planets during the excitation of the Kuiper Belt, as in the NICE model (*Tsiganis et al.*, 2005). Also, satellitesimals may be accreted onto the planet or lost by an evection resonance (*Nesvorný et al.* 2003).

The timescale constraint imposed by Callisto’s partially differentiated state requires that the mutual collision probability between the largest satellitesimals in the circumplanetary disk must be sufficiently low in order not to capture too much mass too quickly. In order to avoid differentiation, Callisto must form in $\gtrsim 10^5$ years, so that the feeding timescale of planetesimals should be at least this long. Thus, a characteristic of the planetesimal capture scenario that satisfies the Callisto constraint is that the mass of the extended disk of solids at any one time (excluding satellite embryos) is typically a small fraction of a Galilean satellite (*Estrada and Mosqueira*, 2006).

Collisions in the circumplanetary disk can lead to fragmentation, accretion, or the removal of material from the outer to the inner portions of the disk, where the satellites form. This collisional removal of material (to the inner disk) is assumed to be replenished by the collisional capture of heliocentric planetesimal fragments. Removal of material from the outer regions to the inner regions can occur because the net specific angular momentum of the satellitesimal swarm (which consists of both retrograde and prograde satellitesimals) is consistent with a much more compact disk.

Initially, the specific angular momentum ℓ_z is quite small, but as the planet begins to clear its feeding zone, sufficient planetesimals are fed from the outermost regions of the feeding zone where inhomogeneities in the circumsolar planetesimal disk increases ℓ_z of the circumplanetary swarm significantly (*Lissauer and Kary*, 1991; *Dones and Tremaine*, 1993; *Estrada and Mosqueira*, 2006), whether they are captured or not (see below). *Estrada and Mosqueira* (2006) posited that these collisional processes may possibly deliver enough ℓ_z to properly account for the total mass and angular momentum contained in the Galilean satellites, but required more detailed calculations in order to demonstrate it.

4.4.2. Angular Momentum Delivery. In order to demonstrate that the proper angular momentum can be delivered over the satellite accretion timescale, *Estrada and Mosqueira* (2006) explore solutions using a detailed analysis that simultaneously satisfies the mass and angular momentum constraints. In their calculations, it is assumed that the bulk of the angular momentum arrives late as the planet clears its feeding zone, and that the planetesimal population is composed of smaller particles $\lesssim 1$ km (e.g., due to collisional grinding, Sec. 4.2). The planetesimal velocity dispersion used is characteristic of a fairly cold population ($\theta \sim 100$) with lower inclinations than eccentricities (e.g., *Ohtsuki and Ida*, 1998). One such calculation for different values of the angular momentum deposition efficiency ϵ is shown in the left panel of Figure 9 for the total angular momentum L_z and mass M , and the right panel of Fig. 9 for the specific angular momentum ℓ_z scaled to the actual value of the Galilean satellite system. In the left panel, these solutions correspond to the locations where the related mass and angular momentum curves intersect (denoted by a pointer). In these calculations, a planetesimal capture probability as a function of disk radius $p(R)$ is used (*Ruskol*, 1975; *Estrada and Mosqueira*, 2006) such that $p(R) \lesssim \epsilon$. This is meant to take into account that, on average, a collision between an incoming planetesimal and satellitesimal may deposit a significant amount of angular momentum in the disk even if they (or their fragments) are not captured.

Solutions in Fig. 9 were found for a range of gap sizes in the heliocentric planetesimal population, $R_{gap} \sim 0.5 - 1.5 R_H$. In this case, a gap refers to a depletion of solids in the circumsolar disk,

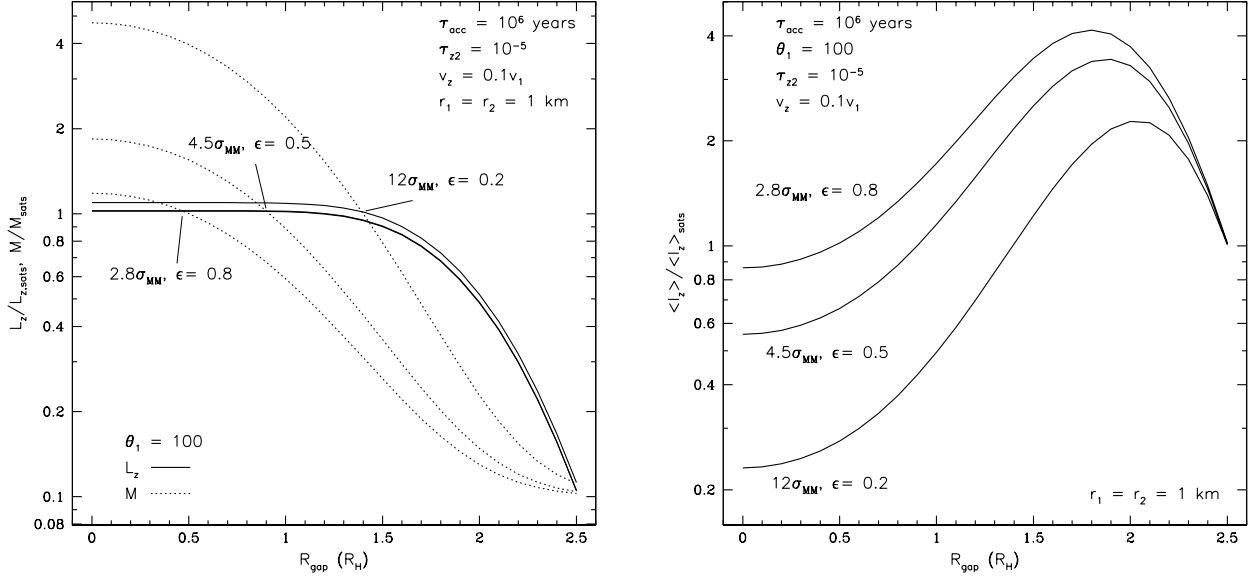


Figure 9: Left: Mass (dotted lines) and angular momentum (solid lines) normalized to the values characteristic of the Galilean satellites ($M_{\text{sats}} \sim 4 \times 10^{26}$ g, $L_{z,\text{sats}} \sim 4 \times 10^{43}$ g cm² s⁻¹) delivered to the circumplanetary disk in $\tau_{\text{acc}} = 10^6$ years as a function of gap size. Solutions for the given parameters are indicated by a pointer to where corresponding lines of M and L_z intersect. Right: Corresponding solutions for the specific angular momentum. In these plots, the “optical depth” τ_{z2} is the collision probability between the largest satellitesimals in the circumplanetary disk, and the planetesimal scale height is $\sim v_z/\Omega$. See *Estrada and Mosqueira, 2006* for details.

analogous to a gas gap. As can be seen from Fig. 9 (right panel), the specific angular momentum contribution increases as the solids gap grows larger. However, the total amount of mass and angular momentum that can be delivered is limited by the size of the planet’s feeding zone, roughly $R_{\text{gap}} \sim 2.5R_H$. Thus, the angular momentum is seen to reach a maximum before beginning to decrease sharply as the gap size chokes off the mass inflow. The mass inflow will drop to nearly zero *unless* there are mechanisms that can replenish the feeding zone of solids material.

The results suggest that it may be possible to deliver enough mass and angular momentum to the Jovian system to explain the Galilean satellites. In order to satisfy the Callisto constraint, however, the timescale over which planetesimal fragments are fed into the system needs to extend over $\sim 10^5 - 10^6$ years, which may be problematic given that the feeding timescale of planetesimals may be $\sim 10^5$ years (or less, Sec. 4.2). The implication is that one may have to replenish the feeding zone of the giant planet with planetesimal fragments brought in by gas drag. This seems quite possible given there are plausible mechanisms that can lead to local nebula solids enhancement (e.g., see Sec. 2.4). Given that a necessary criterion for finding the solutions in Fig. 9 is that the solar nebula is enhanced in solids over that of the standard MMSN at the location of Jupiter, a continuous replenishment mechanism may not be unrealistic. However, further work will need to be done to assess whether it is feasible to deliver material over such a long timescale. The alternative is that Callisto is differentiated (See Sec. 4.5), in which case the timescale constraints for formation of the satellites are invalidated.

4.5. Satisfying the Constraints

4.5.1. The Compositional Gradient. There are two predominant explanations for this observation. The first ascribes the high-silicate fraction of Europa relative to Ganymede and Callisto to the subnebula temperature gradient due to Jupiter’s luminosity at the time of satellite formation (e.g., *Pollack et al.*, 1976; *Lunine and Stevenson*, 1982). In this view, Ganymede’s temperature is typically set at $T \sim 250\text{K}$ to allow for the condensation of ice at its location. Closer in, a persistently hot subnebula would prevent the condensation of volatiles close to Jupiter (*Pollack and Reynolds*, 1974; *Lunine and Stevenson*, 1982), possibly over the lifetime of the disk because Jovian disk cooling times are comparable to disk dissipation times. In the optically thick case, this implies a planetary luminosity $\sim 10^{-5} L_{\odot}$ (where $L_{\odot} = 3.827 \times 10^{33} \text{ ergs s}^{-1}$ is the solar luminosity) for a planetary radius of $1.5 - 2 R_J$ (e.g., Fig. 1). But, it is important to keep in mind that other possible fractionation mechanisms include tidal heating, which may apply to Io and Europa (and Enceladus in the Saturnian system), and impact driven devolatilization, which would weaken the basis for this constraint. In particular, Io can lose its volatiles due to the Laplace resonance alone.

However, this picture may run into trouble because the inner small satellite Amalthea (located at $\sim 1.4 R_J$, Io is at $\sim 6 R_J$) has such a low mean density (0.86 g cm^{-3}) that models for its composition require that water-ice be a major constituent, even for improbably high values of porosity (*Anderson et al.*, 2005). If the increase in ice fraction with distance came by as a result of Jupiter’s luminosity, then it would require that Amalthea is either a captured object, formed elsewhere and was subsequently delivered to the inner disk by some dynamical process, or is a rocky object that has a highly improbable internal structure and/or accretion scenario.

The second explanation argues that the compositional gradient may be due to the increase of impact velocities and impactor flux of Roche-lobe interlopers deep in the planetary potential well, leading to preferential volatile depletion in the case of Io, and Europa (*Shoemaker*, 1984). In this view, all of the Galilean satellites would start out ice-rich, but some would lose more volatiles than others. Given that the mid-sized Saturnian satellites may provide an observational confirmation of such a process, one might expect a stochastic compositional component deep in the planetary potential well due to high speed $\gtrsim 10 \text{ km s}^{-1}$ impacts with large (perhaps $\sim 10 - 100 \text{ km}$) Roche-lobe interlopers. Such hyperbolic collisions might conceivably remove volatiles from the mantle of a differentiated satellite and place them on neighboring satellites. This might then explain the volatile depletion in Europa relative to Ganymede and Callisto. A similar argument may apply to Enceladus in the Saturnian system. Amalthea then may be a collisional remnant of this process. The gas-poor satellite accretion environment (Sec. 4.4) is most consistent with this scenario, although a stochastic component is by no means excluded from the gas-rich scenario.

4.5.2. The Callisto Constraint. If Callisto is partially differentiated, it argues that Callisto’s formation took place over a timescale $\gtrsim 10^5$ years (*Mosqueira et al.*, 2001; *Mosqueira and Estrada*, 2003a,b; *Canup and Ward*, 2002; *Alibert et al.*, 2005a; *Estrada and Mosqueira*, 2006). A long formation timescale may be required because the energy of accretion must be radiated away (*Safronov*, 1969; *Stevenson et al.*, 1986) to avoid melting the interior. However, proper treatment of this problem needs to include the effects of an atmosphere (*Kuramoto and Matsui*, 1994), which allows for hydrodynamic blow-off, or convective transport to the subnebula. Yet, non-hydrostatic mass anomalies at the boundary of the rocky core could still imply a differentiated state (*McKinnon*, 1997; *Stevenson et al.*, 2003).

Assuming hydrostatic equilibrium, the simplest interpretation for Callisto’s moment of inertia is a satellite structure consisting of a 300 km rock-free ice shell over a homogeneous rock and ice interior (*Anderson et al.*, 2001; *Schubert et al.*, 2004). If Callisto’s internal structure is primordial, and it was accreted homogeneously, impacts during the late-stages of its growth can be used to raise the temperature of the surface regions of the satellite to the melting point and to supply the latent

heat of melting (and vaporization), possibly leading to partial differentiation of just the surface layers.

On the other hand, the energy liberated by the sinking rocky component can eventually lead to a runaway process (*Friedson and Stevenson, 1983*). Moreover, both radiogenic heating and the presence of ammonia in the interior can result in a more stringent constraint on Callisto’s thermal history. However, the relevance of these factors is uncertain if Callisto is indeed only partially differentiated: although ammonia may help to sustain an ocean in Callisto (inferred to be present from Galileo magnetometer data; *Zimmer et al., 2000*), salts concentrated in the liquid layer and/or a satellite surface regolith can also help in this regard (*Spohn and Schubert, 2003*); and the addition of ^{26}Al , as specified by carbon-aluminum inclusions (CAIs), depends on the assumption of spatial and temporal homogeneity (see *Wadhwa et al., 2007* and references therein; *Castillo-Rogez et al., 2007*). We stress that the likely presence of an ocean means that melting did take place, presumably during satellite accretion. Furthermore, the possible presence of ammonia need not result in full differentiation (*Ellsworth and Schubert, 1981*).

A number of explanations for the Callisto-Ganymede dichotomy have been offered that rely on fine-tuning uncertain parameters (*Schubert et al., 1981; Lunine and Stevenson, 1982; Friedson and Stevenson, 1983; Stevenson et al., 1986*). *Showman and Malhotra (1997)* proposed an explanation based on the Laplace resonance; yet, it is unclear that Ganymede could have suffered sufficient tidal heating to explain the differences between the two satellites.

The differences between Ganymede and Callisto can be a consequence of the disk formation and evolution scenario described in Sec. 4.3 in which Callisto’s formation time is very long compared to that of Ganymede. In this gas-rich environment, Callisto’s accretion timescale is tied to the disk clearing timescale ($\sim 10^6$ years; *Mosqueira and Estrada, 2003a*). That is, in this view Callisto derives its full mass from satellitesimals in the extended outer disk that are brought into its feeding by gas drag migration. On the other hand, because Callisto poses an effective barrier for inwardly migrating objects, Ganymede must derive most of its mass from a more compact, denser region inside of Callisto’s orbit, resulting in a much shorter accretion timescale ($\lesssim 10^4$ years). This means that while Callisto may have enough time to radiate away its energy of accretion Ganymede does not. This explanation for the Ganymede-Callisto dichotomy does not require special pleading for Callisto, but rather relies on its outer location to explain its accretional and thermal history. Note that a similar formation timescale would apply to Iapetus in the Saturnian system for the same reason, i.e., its outermost location would lead to long disk clearing times, which is directly tied to the satellite accretion time.

An additional concern is whether impacts with large embryos could result in Callisto’s differentiation (*McKinnon, 2006*). In the SEMM model, typical radii of inwardly migrating embryos that form in the outer disk are $\sim 200 - 500$ km. However, these embryo sizes should *not* be confused with the typical sizes of the objects that accrete onto Callisto. Characterizing typical impactor sizes requires treatment of the interaction between a late-stage protosatellite and a swarm of satellitesimals, including the effects of collisional fragmentation.

Work by *Weidenschilling and Davis, (1985)* shows that a combination of gas drag and perturbations due to mean motion resonances with a planet (or satellite) has important consequences for the evolution of planetesimals (or satellitesimals/embryos). Inwardly migrating embryos can be readily captured into resonance before reaching Callisto (note that Hyperion is in such a resonance with Titan). *Malhotra (1993)* points out, though, that resonance trapping is vulnerable to mutual planetesimal (or satellitesimal) interactions, so that as the embryos approach a satellite collisions among the embryos are expected to be destructive (see *Agnor and Asphaug, 2004* for an analogous argument for planets), grinding them down and knocking them out of resonance. In this view,

Hyperion (radius ~ 150 km) might represent a collisional remnant or survivor of such a collisional cascade. It is reasonable to expect that Hyperion-like or smaller objects might be typical impactors in the late-stage formation of Callisto (and Titan). Furthermore, one might expect such impactors to be porous, of low density (~ 0.5 g cm $^{-3}$), and likely undifferentiated, all of which tend to favor shallower energy deposition during satellite accretion. The question then becomes whether Callisto’s $\sim 10^6$ year accretion from Hyperion-like (or smaller), porous impactors striking the satellite at its escape speed would result in a partially differentiated state. This problem remains to be tackled in detail.

Alternatively, models that make Ganymede and Callisto in the same timescale rely on fine-tuning unknown parameters to explain the differences between these two satellites. This also applies to the gas-poor (GPPC) model, which forms both Callisto and Ganymede by the delivery of small collisional fragments and debris to the circumplanetary disk over a long timescale. Yet, the planetesimal clearing timescale in the Jupiter-Saturn region is $\lesssim 10^5$ years (*Charnoz and Morbidelli, 2003*). Note that in the NICE model (*Tsiganis et al., 2005*), the timescale for planetesimal delivery could be even shorter since Jupiter and Saturn are initially closer together. Therefore in the GPPC model a challenge is to deliver enough mass at later times to lead to the formation of a partially differentiated Callisto. Possible ways to lengthen the planetesimal delivery timescale include stirring of the circumsolar disk by Uranus and Neptune, and planetesimal replenishment by gas-drag inward migration of meter-sized bodies.

In conclusion, it is important to point out that neither of the disk models discussed in Sections 4.3 and 4.4 hinge on Callisto’s internal state. If Callisto turns out to be differentiated, both models remain viable because neither hinges on a long accretion timescale.

5. SUMMARY

We have attempted to provide a broad picture of the origin of the Jovian system from its humble beginnings with the accumulation of the first generation of planetesimals, to the birth of the magnificently complex system we see today. We have done so by summarizing our current understanding of the various stages of Jupiter’s formation with the support of the most current numerical models of its accretion. There are several issues that still need to be squared away in models that treat Jupiter’s growth in isolation (see, *Lissauer and Stevenson, 2007*); most notably, more realistic opacity models for the giant planet envelope need to be implemented (e.g. *Movshovitz and Podolak, 2007*), and while we did not touch upon this subject in regards to the planets, the type I migration rate of a growing protoplanet remains a subject of debate. Both issues are intimately tied to requirement that Jupiter form faster than the nebula dispersal time. However, the level of sophistication in these growth models continues to increase, with efforts to marry models that form giant planets in isolation to simulations of embedded planets in circumstellar disks just beginning to be explored (*Hubickyj et al., 2007*).

We have further identified where the circumplanetary disk, a by-product of Jupiter’s later stages of accretion, fits into Jupiter’s formation history. There are two components to this disk: a more radially compact disk that forms as a result of the accretion of low specific angular momentum gas during a period after envelope contraction and prior to opening a deep gap in the solar nebula; and, a more radially extended disk which arises as a result of continued gas inflow through a deep gap as Jupiter approaches its final mass. The resulting disk may be initially massive as one might expect from a rough equipartition of angular momentum between itself and the planet (e.g., *Stevenson et al., 1986*), but is expected to evolve (driven by the inflow) at least until the gas inflow wanes. A massive disk may play a key role in determining the final spin angular momentum of Jupiter.

Presently, planetary formation models tend to focus on either the growth of the planet in the spherically symmetric approximation, or a protoplanet embedded in a circumstellar disk in the presence of a well formed gap. As a result, our understanding of the formation of the circumplanetary disk remains incomplete, because no simulations yet exist that model disk formation from envelope contraction to the isolation of the giant planet, when accretion ends. Thus caution must be exercised in interpreting current numerical results. One important result that we may acknowledge from recent numerical simulations, however, is that the size of the circumplanetary disk formed is dependent on the specific angular momentum of the gas flowing into the planet's Roche lobe, and thus whether a deep gap is present or not. Gap-opening likely happens towards the tail end the runaway gas accretion phase as Jupiter approaches its final mass. If the architecture of the Solar System were such that Saturn began much closer to Jupiter (as in the NICE model, *Tsiganis et al.*, 2005), disk truncation would be accomplished jointly.

How the circumjovian gas disk evolves over time is dependent on the level of both solar nebula and subnebula turbulence. It is expected that as long as there is inflow through the giant planet gap, it will drive subnebula evolution. However, whether or not there is an intrinsic source of turbulence in the circumplanetary disk has a profound effect on the environment in which the Galilean satellites formed. We have offered examples of different pathways to satellite growth and survival dependent on whether one posits sustained turbulence, or turbulence decay once the inflow subsides. The assumption leads to two qualitatively different formation environments. Both explain the angular momentum of the regular satellites, yet neither is restricted by necessity to satisfy the Callisto constraint. That is, both models can allow for a differentiated or partially differentiated Callisto, because neither depends on Callisto having a long formation timescale. In addition, both models rely on planetesimal delivery mechanisms to provide the mass necessary to form the satellites, and do not rely on dust inflow, which by itself necessarily implies long formation times. The apparent compositional diversity and potential similarities in the primordial compositions of the satellites of Jupiter and Saturn (*Hibbitts*, 2006) hint that Jupiter and its satellite system may be composed of planetesimals formed locally as well as in more distant regions of the solar nebula. The overall implication then is that planetesimal delivery mechanisms likely provide the bulk of material for satellite accretion, regardless of the gas mass contained in the circumjovian disk.

Finally, as the inventory of discovered extrasolar planets increases, the discussion within this chapter gains in relevance. Despite, in most cases, there being clear dynamical differences between these newly discovered planetary systems and our own, having an understanding of Jupiter's formation from its beginning to its late stages still serves as an essential benchmark to our general understanding of giant planet formation, and, by analogy, of the formation of the satellite systems which likely await as secondary discoveries around these extrasolar giants.

REFERENCES

- Agnor, C. B., Canup, R. M., and Levison, H. F. (1999) On the Character and Consequences of Large Impacts in the Late Stage of Terrestrial Planet Formation. *Icarus*, 142, 219-237.
- Agnor, C. B., and Asphaug, E. (2004) Accretion efficiency during planetary collisions. *Astrophys. J.*, 613, L157-L160.
- Agnor, C. B., and Hamilton, D. P. (2006) Neptune's capture of its moon Triton in a binary-planet gravitational encounter. *Nature*, 441, 192-194.
- Alibert, Y., Mousis, O., Benz, W. (2005a) Modeling the Jovian subnebula. I. Thermodynamical conditions and migration of proto-satellites. *Astron. Astrophys.*, 439, 1205-1213.
- Alibert, Y., Mousis, O., Mordasini, C. and Benz, W. (2005b) New Jupiter and Saturn Formation Models Meet Observations. *Astrophys. J.*, 626, L57-L60.

- Anderson, J. D., Schubert, G., Jacobson, R. A., Lau, E. L., Moore, W. B., and Sjogren, W. L. (1998) Distribution of rock, metals, and ices in Callisto. *Science*, 280, 1573-1576.
- Anderson, J. D., Jacobson, R. A., McElrath, T. P., Moore, W. B., Schubert, G., and Thomas, P. C. (2001) Shape, mean radius, gravity field, and interior structure of Callisto. *Icarus*, 153, 157-161.
- Anderson, J. D., and 11 colleagues (2005) Amalthea's density is less than that of water. *Science*, 308, 1291-1293.
- Andrews, S. M., and Williams, J. P. (2007) High-resolution submillimeter constraints on circumstellar disk structure. *Astrophys. J.*, 659, 705-728.
- Artymowicz, P., and Lubow, S. H. (1996) Mass flow through gaps in circumbinary disks. *Astrophys. J.*, 467, L77-L80.
- Afshordi, N., Mukhopadhyay, B., and Narayan, R. (2005) Bypass to turbulence in hydrodynamic accretion: Lagrangian analysis of energy growth. *Astrophys. J.*, 629, 373-382.
- Atreya, S. K., Wong, M. H., Owen, T. C., Mahaffy, P. R., Niemann, H. B., de Pater, I., Drossart, P., and Encrenaz, T. (1999) A comparison of the atmospheres of Jupiter and Saturn: Deep atmospheric composition, cloud structure, vertical mixing, and origin. *Planet. Space. Sci.*, 47, 1243-1262.
- Balbus, S. A., and Hawley, J. F. (1991) A powerful local shear instability in weakly magnetized disks. II. Nonlinear evolution. *Astrophys. J.*, 376, 223.
- Balbus, S. A., Hawley, J. F., and Stone, J. M. (1996) Nonlinear stability, hydrodynamical turbulence, and transport in disks. *Astrophys. J.*, 467, 76.
- Bar-Nun, A., Herman, G., Laufer, D., and Rappaport, M. L. (1985) Trapping and release of gases by water ice and implications for icy bodies. *Icarus*, 63, 317-332.
- Bar-Nun, A., Dror, J., Kochavi, E., and Laufer, D. (1987) Amorphous water ice and its ability to trap gases. *Phys. Rev. B*, 35, 2427-2435.
- Bar-Nun, A., Kleinfeld, I., and Kochavi, E. (1988) Trapping of gas mixtures by amorphous water ice. *Phys. Rev. B*, 38, 7749-7754.
- Bar-Nun, A., Notesco, G., and Owen, T. (2007) Trapping of N₂, CO and Ar in amorphous ice Application to comets. *Icarus*, 190, 655-659.
- Barranco, J. A., and Marcus, P. S. (2005) Three-dimensional Vortices in Stratified Protoplanetary Disks. *Astrophys. J.*, 623, 1157-1170.
- Bate, M. R., Ogilvie, G. I., Lubow, S. H., and Pringle, J. E. (2002) The excitation, propagation, and dissipation of waves in accretion disks: the non-linear axisymmetric case. *Mon. Not. Roy. Astron. Soc.*, 332, 575-600.
- Bate, M. R., Lubow, S. H., Ogilvie, G. I., and Miller, K. A. (2003) Three-dimensional calculations of high- and low-mass planets embedded in protoplanetary disks. *Rev. Modern Phys.*, 70, 1-53.
- Bell, K. R., and Lin, D. N. C. (1994) Using FU Orionis outbursts to constrain self-regulated protostellar disk models. *Astrophys. J.*, 427, 987-1004.
- Bodenheimer, P., and Pollack, J. B. (1986) Calculations of the accretion and evolution of the giant planets: the effects of solid cores. *Icarus*, 67, 391-408.
- Bodenheimer, P., Burkert, A., Klein, R. and Boss, A.P. (2000) Multiple Fragmentation of Protostars. In *Protostars and Planets IV* (V. Mannings, A. P. Boss, and S. S. Russell, eds.), pp. 675-701. University of Arizona Press, Tucson.
- Boss, A. P. (2000) Gas Giant Protoplanet Formation: Disk Instability Models with Thermodynamics and Radiative Transfer. *Astrophys. J.*, 536, L101-L104.
- Boynnton, W. V. (1985) Meteoritic evidence concerning conditions in the solar nebula. In *Protostars and Planets II*, (D. C. Black, M. S. Matthews, eds.), pp. 772-790. University of Arizona Press, Tucson.

- Brownlee, D., and 182 colleagues (2006) Comet 81P/Wild 2 under a microscope. *Science*, 314, 1711-1716.
- Bryden, G., Chen, X., Lin, D. N. C., Nelson, R. P., and Papaloizou, C. B. (1999) Tidally induced gap formation in protostellar disks: Gap clearing and suppression of protoplanetary growth. *Astrophys. J.*, 514, 344-367.
- Bryden, G., Rozyczka, M., Lin, D. N. C., and Bodenheimer, P. (2000) On the interaction between protoplanets and protostellar disks. *Astrophys. J.*, 540, 1091-1101.
- Buriez, J. C., and de Bergh, C. (1981) A study of the atmosphere of Saturn based on methane line profiles near 1.1 microns. *Astron. Astrophys.*, 94, 382-390.
- Cai, K., Durisen, R. H., Michael, S., Boley, A. C., Meja, A. C., Pickett, M. K., and D'Alessio, P. (2006) The effects of metallicity and grain size on gravitational instabilities in protoplanetary disks. *Astrophys. J.*, 636, L149-L152.
- Cameron, A. G. W., Decampli, W. M., and Bodenheimer, P. (1982) Evolution of giant gaseous protoplanets embedded in the primitive solar nebula. *Icarus*, 49, 298-312.
- Canup, R., and Ward, W. R. (2002) Formation of the Galilean satellites: Conditions for accretion. *Astron. J.*, 124, 3404-3423.
- Cassen, P., and Pettibone, D. (1976) Steady accretion of a rotating fluid. *Astrophys. J.*, 208, 500-511.
- Castillo-Rogez, J. C., Matson, D. L., Sotin, C., Johnson, T. V., Lunine, J. I., and Thomas, P. C. (2007) Iapetus' geophysics: Rotation rate, shape, and equatorial ridge. *Icarus*, 190, 179-202.
- Chagelishvili, G. D., Zahn, J.-P., Tevzadze, A. G., and Lominadze, J. G. (2003) On hydrodynamic shear turbulence in Keplerian disks: Via transient growth to bypass transition. *Astron. Astrophys.*, 402, 401-407.
- Chambers, J. E. (2001) Making more terrestrial planets. *Icarus*, 152, 205-224.
- Charnoz, S. and Morbidelli, A. (2003) Coupling dynamical and collisional evolution of small bodies: An application to the early ejection of planetesimals from the Jupiter-Saturn region. *Icarus*, 166, 141-156.
- Chiang, E. I., and Goldreich, P. (1997) Spectral energy distributions of T Tauri stars with passive circumstellar disks. *Astrophys. J.*, 490, 368-376.
- Ciesla F. J., and Cuzzi, J. N. (2006) The evolution of the water distribution in a viscous protoplanetary disk. *Icarus*, 81, 178-204.
- Ciesla, F. J. (2007) Outward transport of high-temperature materials around the midplane of the solar nebula. *Science*, 318, 613-616.
- Clark, R. N., and 24 colleagues (2005) Cassini VIMS compositional mapping of surfaces in the Saturn system and the role of water, cyanide compounds and carbon dioxide (abstract). In *BAAS*, 37, abstract # 39.05, pp. 701.
- Clayton, R. N., Mayeda, T. K., and Molina-Velsko, C. A. (1985) Isotopic variations in solar system material: Evaporation and condensation of silicates. In *Protostars and Planets II*, (D. C. Black, M. S. Matthews, eds.), pp. 755-771. University of Arizona Press, Tucson.
- Clayton, R. N. (1993) Oxygen isotopes in meteorites. *Annual Rev. Astron. Astrophys.*, 21, 115-149
- Clayton, R. N. (2003) Oxygen isotopes in the solar system. *Spa. Sci. Rev.*, 106, 19-32.
- Cody, G. D., Yabuta, H., Alexander, C. M. O'd., Araki, T., and Kilcoyne, A. L. D. (2007) Placing comet 81P/Wild 2 Ooganic particles into context with chondritic organic solids (abstract). In *Lunar and Planetary Science XXXVIII*, Abstract # 1338, Lunar and Planetary Institute, Houston (CD-ROM).
- Coradini, A., Magni, G., and Federico, C. (1981) Gravitational instabilities in satellite disks and formation of regular satellites. *Astron. Astrophys.*, 99, 255-261.

- Coradini, A., Federico, C., and Luciano, P. (1982) Ganymede and Callisto: Accumulation heat content. In *The Comparative Study of Planets*, (A. Coradini, and N. Fulchignoni, eds.), Dordrecht Reidel, Dordrecht.
- Coradini, A., Cerroni, P., Magni, G., and Federico, C. (1989) Formation of the satellites of the outer solar system - Sources of their atmospheres. In *Origin and Evolution of Planetary and Satellite Atmospheres*, (S. K. Atreya, J. B. Pollack, and M. S. Matthews, eds.), pp. 723-762, University of Arizona Press, Tucson.
- Courtin, R., Gautier, D., Marten, A., Bezard, B., and Hanel, R. (1984) The composition of Saturn's atmosphere at northern temperate latitudes from Voyager IRIS spectra - NH_3 , PH_3 , C_2H_2 , C_2H_6 , CH_3D , CH_4 , and the Saturnian D/H isotopic ratio. *Astrophys. J.*, 287, 899-916.
- Cruikshank, D. P., and 23 colleagues (2005) Aromatic Hydrocarbons on Iapetus and Phoebe: Cassini-VIMS Detections (abstract). In *BAAS*, 37, abstract # 39.06, pp. 705.
- Cruikshank, D. P., and 30 colleagues (2007a) Surface composition of Hyperion. *Nature*, 448, 54-56.
- Cruikshank, D. P., and 27 colleagues (2007b) Hydrocarbons on Saturn's satellites Iapetus and Phoebe. *Icarus*, in press.
- Cuzzi, J. N., Dobrovolskis, A. R., and Champney, J. M. (1993) Particle-gas dynamics in the mid-plane of the protoplanetary nebula. *Icarus*, 106, 102-134.
- Cuzzi, J. N., Davis, S. S., and Dobrovolskis, A. R. (2003) Radial drift, evaporation, and diffusion: enhancement and redistribution of silicates, water, and other condensibles in the nebula (abstract). In *BAAS*, 35, # 27.02, pp. 964.
- Cuzzi, J. N., and Hogan, R. C. (2003) Blowing in the wind I. Velocities of chondrule-sized particles in a turbulent protoplanetary nebula. *Icarus*, 164, 127-138.
- Cuzzi, J. N., and Zahnle, K. J. (2004) Material enhancement in protoplanetary nebulae by particle drift through evaporation fronts. *Astrophys. J.*, 614, 490-496.
- Cuzzi, J. N., and Weidenschilling, S. J. (2004) Formation of planetesimals in the solar nebula. In *Protostars and Planets III*, ((E. H. Levy, and J. I. Lunine, eds.), pp. 1031-1060, University of Arizona Press, Tucson.
- Cuzzi, J. N., Ciesla, F. J., Petaev, M. I., Krot, A. N., Scott, E. R. D., and Weidenschilling, S. J. (2005) Nebula evolution of thermally Pprocessed solids: Reconciling models and meteorites. In *Chondrites and the Protoplanetary Disk*, (A. N. Krot, E. R. D. Scott, and B. Reipurth, eds.), pp. 732, Astronomical Society of the Pacific.
- Cuzzi, J. N., and Weidenschilling, S. J. (2006) Particle-gas dynamics and primary accretion. In *Meteorites and the Early Solar System II*, (D. S. Lauretta and H. Y. McSween Jr., eds.), pp. 353-381, University of Arizona Press, Tucson.
- Cuzzi, J. N., Hogan, R. C., and Shariff, K. (2007) Towards a scenario for primary accretion of primitive bodies (abstract). In Lunar and Planetary Science XXXVIII, Abstract # 1338, Lunar and Planetary Science Institute, Houston (CD-ROM).
- D'Angelo, G., Henning, T., and Kley, W. (2002) Nested-grid calculations of disk-planet interaction. *Astron. Astrophys.*, 385, 647-670.
- D'Angelo, G., Kley, W. and Henning, T. (2003a) Orbital Migration and Mass Accretion of Protoplanets in Three-dimensional Global Computations with Nested Grids. *Astrophys. J.*, 586, 540-561.
- D'Angelo, G., Henning, T., and Kley, W. (2003b) Thermohydrodynamics of circumstellar disks with high-mass planets. *Astrophys. J.*, 599, 548-576.
- D'Angelo, G., Bate, M. R., and Lubow, S. H. (2005) The dependence of protoplanet migration rates on co-orbital torques. *Mon. Not. Roy. Astron. Soc.*, 358, 316-332.
- de Pater, I., and Massie, S. T. (1985) Models of the millimeter-centimeter spectra of the giant planets. *Icarus*, 62, 143-171.

- Dominik, C., Blum, J., Cuzzi, J. N., and Wurm, G. (2007) Growth of dust as the initial step toward planet formation. In *Protostars and Planets V*, (B. Reipurth, D. Jewitt, and K. Keil, eds.), pp. 783-800. University of Arizona Press, Tucson.
- Dones, L., and Tremaine, S. (1993) On the origin of planetary spins. *Icarus*, 103, 67-92.
- Dullemond, C. P., and Dominik, C. (2005) Dust coagulation in protoplanetary disks: A rapid depletion of small grains. *Astron. Astrophys.*, 434, 971-986.
- Dullemond, C. P., Hollenbach, D., Kamp, I., and D'Alessio, P. (2007) Models of the structure and evolution of protoplanetary disks. In *Protostars and Planets V*, (B. Reipurth, D. Jewitt, and K. Keil, eds.), pp. 559-572. University of Arizona Press, Tucson.
- Durisen, R. H., Boss, A. P., Mayer, L., Nelson, A. F., Quinn, T., and Rice, W. K. M. (2007) Gravitational instabilities in gaseous protoplanetary disks and implications for giant planet formation. In *Protostars and Planets V*, (B. Reipurth, D. Jewitt, and K. Keil, eds.), pp. 607-622. University of Arizona Press, Tucson.
- Dutrey, A., Guilloteau, S., Duvert, G., Prato, L., Simon, M., Schuster, K., and Menard, F. (1996) Dust and gas distribution around T Tauri stars in Taurus-Auriga. I. Interferometric 2.7mm continuum and ^{13}CO J=1-0 observations. *Astro. Astrophys.*, 309, 493-504.
- Estrada, P. R. (2002) Formation of satellites around gas giant planets. Ph.D. thesis, Cornell University, Ithaca. 326 pp.
- Estrada, P. R., and Mosqueira, I. (2006) A gas-poor planetesimal capture model for the formation of giant planet satellite systems. *Icarus*, 181, 486-509.
- Friedson, A. J., and Stevenson, D. J. (1983) Viscosity of rock-ice mixtures and applications to the evolution of icy satellites. *Icarus*, 56, 1-14.
- Gammie, C. F. (1996) Linear theory of magnetized, viscous, self-gravitating gas disks. *Astrophys. J.*, 463, 725.
- Gammie, C. F., and Johnson, B. M. (2005) Theoretical studies of gaseous disk evolution around solar mass stars. In *Chondrites and the Protoplanetary Disk*, (A. N. Krot, E. R. D. Scott, and B. Reipurth., eds.), ASP Conference Series, 341, pp. 145.
- Garaud, P., and Lin, D. N. C. (2007) The Effect of Internal Dissipation and Surface Irradiation on the Structure of Disks and the Location of the Snow Line around Sun-like Stars. *Astrophys. J.*, 654, 606-624.
- Gautier, D. Hersant, F., Mousis, O., and Lunine, J. I. (2001a) Enrichments in volatiles in Jupiter: A new interpretation of the Galileo measurements. *Astrophys. J.*, 550, L227-L230.
- Gautier, D. Hersant, F., Mousis, O., and Lunine, J. I. (2001b) Erratum: Enrichments in volatiles in Jupiter: A new interpretation of the Galileo measurements. *Astrophys. J.*, 559, L183.
- Gladman, B. and Duncan, M. (1990) On the fates of minor bodies in the outer solar system. *Astron. J.*, 100, 1680-1693.
- Goldreich, P., and Ward, W. R. (1973) The formation of planetesimals. *Astrophys. J.*, 183, 1051-1062.
- Goldreich, P. and Tremaine, S. (1979) The excitation of density waves at the Lindblad and co-rotation resonances by an external potential. *Astrophys. J.*, 233, 857-871.
- Goldreich, P. and Tremaine, S. (1980) Disk-satellite interactions. *Astrophys. J.*, 241, 425-441.
- Goldreich, P., Lithwick, Y., and Sari, R. (2002) Formation of Kuiper-belt binaries by dynamical friction and three-body encounters. *Nature*, 420, 643-646.
- Goldreich, P., Lithwick, Y., and Sari, R. (2004) Final stages of planet formation. *Astrophys. J.*, 614, 497-507.
- Goodman, J., and Rafikov, R. R. (2001) Planetary torques as the viscosity of protoplanetary disks. *Astrophys. J.*, 552, 793-802.

- Guillot, T. (2005) The interiors of giant planets: Models and outstanding questions. *Annual Rev. Astron. Astrophys.*, 33, 493-530.
- Hawley, J. F., Balbus, S. A., and Winters, W. F. (1999) Local Hydrodynamic Stability of Accretion Disks. *Astrophys. J.*, 518, 394-404.
- Hayashi, C. (1981) Structure of the solar nebula, growth and decay of magnetic fields, and effects of magnetic and turbulent viscosities on the nebula. *Prog. Theor. Phys. Suppl.*, 70, 35-53.
- Hersant, F., Gautier, D., and Lunine, J. I. (2004) Enrichment in volatiles in the giant planets of the Solar System. *Planet. Space Sci.*, 52, 623-641.
- Hibbitts, C. A., McCord, T. B., and Hansen, G. B. (2000) Distributions of CO₂ and SO₂ on the surface of Callisto. *J. Geophys. Res.*, 105, 22541-22558.
- Hibbitts, C. A. (2006) Intriguing differences and similarities in the surface compositions of the icy Saturnian and Galilean satellites (abstract). American Geophysical Union, Fall Meeting 2006, abstract #P32A-08.
- Hibbitts, C. A., Pappalardo, R. T., Hansen, G. B., and McCord, T. B. (2003) Carbon dioxide on Ganymede. *J. Geophys. Res.*, 108, (2)1-22.
- Hill, G. W. (1878) Mr. Hill's paper on the motion of the Moon's perigee. *Mon. Not. R. Astron. Soc.*, 38, 192.
- Hubbard, W. B., Burrows, A., and Lunine, J. I. (2002) Theory of giant planets. *Annual Rev. Astron. Astrophys.*, 40, 103-136.
- Hubickyj, O., Bodenheimer, P., and Lissauer, J. J. (2005) Accretion of the gaseous envelope of Jupiter around a 5-10 Earth-mass core. *Icarus*, 179, 415-431.
- Hubickyj, O., Lissauer, J. J., D'Angelo, G., and Bodenheimer, P. (2007) Formation of Jupiter via core nucleated accretion within a dissipating protoplanetary disk (abstract). American Geophysical Union, Fall Meeting 2007, #P54A-06.
- Ji, H., Burin, M., Scharfman, E., and Goodman, J. (2006) Hydrodynamic turbulence cannot transport angular momentum effectively in astrophysical disks. *Nature*, 444, 343-346.
- Johansen, A., Oishi, J. S., Low, M.-M. M., Klahr, H., Henning, T., and Youdin, A. N. (2007) Rapid planetesimal formation in turbulent circumstellar disks. *Nature*, 448, 1022-1025.
- Kary, D. M., Lissauer, J. J., and Greenszweig, Y. (1993) Nebular gas drag and planetary accretion. *Icarus*, 106, 288.
- Kenyon, S. J., and Hartmann, L. (1987) Spectral energy distributions of T Tauri stars - Disk flaring and limits on accretion. *Astrophys. J.*, 323, 714-733.
- Kenyon, S. J., and Luu, J. X. (1999) Accretion in the Early Outer Solar System. *Astrophys. J.*, 526, 465-470.
- Kitamura, Y., Momose, M., Yokogawa, S., Kawabe, R., Tamura, M., and Ida, S. (2002) Investigation of the physical properties of protoplanetary disks around T Tauri stars by a 1 arcsecond imaging survey: Evolution and diversity of the disks in their accretion stage. *Astrophys. J.*, 581, 357-380.
- Klahr, H. H., and Bodenheimer, P. (2003) Turbulence in accretion disks: Vorticity generation and angular momentum transport via the global baroclinic instability. *Astrophys. J.*, 582, 869-892.
- Klahr, H., and Kley, W. (2006) 3D-radiation hydro simulations of disk-planet interactions. I. Numerical algorithm and test cases. *Astron. Astrophys.*, 445, 747-758.
- Kley, W. (1999) Mass flow and accretion through gaps in accretion discs. *Mon. Not. Roy. Astron. Soc.*, 303, 696-710.
- Kley, W. (2000) On the migration of a system of protoplanets. *Mon. Not. Roy. Astron. Soc.*, 313, L47-L51.
- Kokubo, E., and Ida, S. (1998) Oligarchic Growth of Protoplanets. *Icarus*, 131, 171-178.

- Kornet, K., Rózyczka, M., and Stepinski, T. F. (2004) An alternative look at the snowline in protoplanetary disks. *Astron. Astrophys.*, 417, 151-158.
- Korycansky, D. G., Pollack, J. B., and Bodenheimer, P. (1991) Numerical models of giant planet formation with rotation. *Icarus*, 92, 234-251.
- Kouchi, A., Yamamoto, T., Kozasa, T., Kuroda, T., and Greenberg, J. M. (1994) Conditions for condensation and preservation of amorphous ice and crystallinity of astrophysical ices. *Astron. Astrophys.*, 290, 1009-1018.
- Kuramoto, K., and Matsui, T. (1994) Formation of a hot proto-atmosphere on the accreting giant icy satellite: Implications for the origin and evolution of Titan, Ganymede, and Callisto. *J. Geophys. Res.*, 99, 21183-21200.
- Laskar, J. (2000) On the Spacing of Planetary Systems. *Phys. Rev. Lett.*, 84, 3240-3243.
- Lesur, G., and Longaretti, P.-Y. (2005) On the relevance of subcritical hydrodynamic turbulence to accretion disk transport. *Astron. Astrophys.*, 444, 25-44.
- Levison, H. F., and Morbidelli, A. (2003) The formation of the Kuiper belt by the outward transport of bodies during Neptune's migration. *Nature*, 426, 419-421.
- Li, H., Finn, J. M., Lovelace, R. V. E., and Colgate, S. A. (2000) Rossby wave instability of thin accretion disks. II. Detailed linear theory. *Astrophys. J.*, 533, 1023-1034.
- Lin, D. N. C., and Papaloizou, J. (1979) Tidal torques on accretion discs in binary systems with extreme mass ratios. *Mon. Not. Roy. Astron. Soc.*, 186, 799-812.
- Lin, D. N. C., and Papaloizou, J. (1980) On the structure and evolution of the primordial solar nebula. *Mon. Not. Roy. Astron. Soc.*, 191, 37-48.
- Lissauer, J. J. (1987) Timescales for planetary accretion and the structure of the protoplanetary disk. *Icarus*, 69, 249-265.
- Lissauer, J. J. (1993) Planet formation. *Ann. Rev. Astron. Astrophys.*, 31, 129-174.
- Lissauer, J. J. (1995) Urey prize lecture: On the diversity of plausible planetary systems. *Icarus*, 114, 217-236.
- Lissauer, J. J. (2007) Planets formed in habitable zones of M dwarf stars probably are deficient in volatiles. *Astrophys. J.*, 660, L149-L152.
- Lissauer, J.J., and Kary, D. M. (1991) The origin of the systematic component of planetary rotation. I. Planet on a circular orbit. *Icarus*, 94, 126-159.
- Lissauer, J.J., and Stevenson, D. J. (2007) Formation of giant planets. In *Protostars and Planets V*, (B. Reipurth, D. Jewitt, and K. Keil, eds.), pp. 591-606. University of Arizona Press, Tucson.
- Lubow, S. H., Seibert, M., and Artymowicz, P. (1999) Disk accretion onto high mass planets. *Astrophys. J.*, 526, 1001.
- Lunine, J. I., and Stevenson, D. J. (1982) Formation of the Galilean satellites in a gaseous nebula. *Icarus*, 52, 14-39.
- Lunine, J. I., and Stevenson, D. J. (1985) Thermodynamics of clathrate hydrate at low and high pressures with application to the outer solar system. *Astrophys. J. Supp. Ser.*, 58, 493-531.
- Machida, M. N., Kokubo, E., Inutsuka, S.-I., and Matsumoto, T. (2008) Angular momentum accretion onto a gas giant planet. *Astrophys. J.*, submitted.
- Mahaffy, P. R., Niemann, H. B., Alpert, A., Atreya, S. K., Demick, J., Donahue, T. M., Harpold, D. N., and Owen, T. C. (2000) Noble gas abundance and isotope ratios in the atmosphere of Jupiter from the Galileo Probe Mass Spectrometer. *J. Geophys. Res.*, 105, 15061-15072.
- Makalkin, A. B., Dorofeeva, V. A., and Ruskol, E. L. (1999) Modeling the protosatellite circum-jovian accretion disk: An estimate of the basic parameters. *Solar Sys. Res.*, 33, 456.
- Malhotra, R. (1993) Orbital resonances in the solar nebula - Strengths and weaknesses. *Icarus*, 106, 264-273.

- Marley, M. S., Fortney, J. J., Hubickyj, O., Bodenheimer, P., and Lissauer, J. J. (2007) On the Luminosity of Young Jupiters. *Astrophys. J.*, 541-549.
- Marten, A., Courtin, R., Gautier, D., and Lacombe, A. (1980) Ammonia vertical density profiles in Jupiter and Saturn from their radioelectric and infrared emissivities. *Icarus*, 41, 410-422.
- Mastrapa, R. M. E., and Brown, R. H. (2006) Ion irradiation of crystalline H₂O ice: Effect on the 1.65- μ m band. *Icarus*, 183, 207-214.
- Mayer, L., Quinn, T., Wadsley, J., and Standel, J. (2002) Formation of Giant Planets by Fragmentation of Protoplanetary Disks. *Science*, 298, 1756-1759.
- McKinnon, W. B. (1997) NOTE: Mystery of Callisto: Is it undifferentiated? *Icarus*, 130, 540-543.
- McKinnon, W. B. (2006) Differentiation of the Galilean satellites: It's different out there (abstract). Workshop on Early Planetary Differentiation, LPI Contribution No. 1335, pp. 66-67.
- Mekler, Y., and Podolak, M. (1994) Formation of amorphous ice in the protoplanetary nebula. *Plan. Spa. Sci.*, 42, 865-870.
- Meyer, M. R., Backman, D. E., Weinberger, A. J., and Wyatt, M. C. (2007) Evolution of circumstellar disks around normal stars: Placing our solar system in context. In *Protostars and Planets V*, (B. Reipurth, D. Jewitt, and K. Keil, eds.), pp. 573-590. University of Arizona Press, Tucson.
- Mizuno, H., Nakazawa, K., and Hayashi, C. (1978) Instability of a gaseous envelope surrounding a planetary core and formation of giant planets. *Pro. Theor. Phys.*, 60, 699-710.
- Mizuno, H. (1980) Formation of the Giant Planets. *Prog. Theor. Phys.*, 64, 544-557.
- Morbidelli, A., and Crida, A. (2007) The dynamics of Jupiter and Saturn in the gaseous protoplanetary disk. *Icarus*, 191, 158-171.
- Morfill, G. E., and Völk, H. J. (1984) Transport of dust and vapor and chemical fractionation in the early protosolar cloud. *Astrophys. J.*, 287, 371-395.
- Mosqueira, I., and Estrada, P. R. (2000) Formation of large regular satellites of giant planets in an extended gaseous nebula: Subnebula model and accretion of satellites. Technical Report, NASA Ames Research Center Moffett Field, CA.
- Mosqueira, I., Estrada, P. R., Cuzzi, J. N., and Squyres, S. W. (2001) Circumjovian disk clearing after gap-opening and the formation of a partially differentiated Callisto (abstract). In Lunar and Planetary Science XXXII, Abstract # 1989, Lunar and Planetary Science Institute, Houston.
- Mosqueira, I., and Estrada, P. R. (2003a) Formation of the regular satellites of giant planets in an extended gaseous nebula I: Subnebula model and accretion of satellites. *Icarus*, 163, 198-231.
- Mosqueira, I., and Estrada, P. R. (2003b) Formation of the regular satellites of giant planets in an extended gaseous nebula II: Satellite migration and survival. *Icarus*, 163, 232-255.
- Mosqueira, I., and Estrada, P. R. (2005) On the Origin of the Saturnian Satellite System: Did Iapetus Form In-Situ? (abstract). In Lunar and Planetary Science XXXVI, Abstract # 1951, Lunar and Planetary Institute, Houston (CD-ROM).
- Mosqueira, I., and Estrada, P. R. (2006) Jupiter's obliquity and a long-lived circumplanetary disk. *Icarus*, 180, 93-97.
- Mousis, O., and Gautier, D. (2004) Constraints on the presence of volatiles in Ganymede and Callisto from an evolutionary turbulent model of the Jovian subnebula. *Plan. Spa. Sci.*, 52, 361-370.
- Movshovitz, N., and Podolak, M. (2007) The opacity of grains in protoplanetary atmospheres. *Icarus*, in press.
- Nakagawa, Y., Sekiya, M., and Hayashi, C. (1986) Settling and growth of dust particles in a laminar phase of a low-mass solar nebula. *Icarus*, 67, 375-390.
- Natta, A., Testi, L., Calvet, N., Henning, T., Waters, R., and Wilner, D. (2007) Dust in protoplanetary disks: Properties and evolution. In *Protostars and Planets V*, (B. Reipurth, D. Jewitt, and K. Keil, eds.), pp. 767-782. University of Arizona Press, Tucson.

- Nesvorný, D., Alvarelos, J. L. A., Dones, L., and Levison, H. F. (2003) Orbital and Collisional Evolution of the Irregular Satellites. *Astron. J.*, 126, 398-429.
- Ohtsuki, K., and Ida, S. (1998) Planetary rotation by accretion of planetesimals with nonuniform spatial distribution formed by the planet's gravitational perturbation. *Icarus*, 131, 393-420.
- Ohtsuki, K., Stewart, G. R., and Ida, S. (2002) Evolution of Planetesimal Velocities Based on Three-Body Orbital Integrations and Growth of Protoplanets. *Icarus*, 155, 436-453.
- Ormel, C. W., and Cuzzi, J. N. (2007) Closed-form expressions for particle relative velocities induced by turbulence. *Astron. Astrophys.*, 466, 413-420.
- Ossenkopf, V. (1993) Dust coagulation in dense molecular clouds: The formation of fluffy aggregates. *Astron. Astrophys.*, 280, 617-646.
- Owen, T., and Encrenaz, T. (2003) Element abundances and isotope ratios in the giant planets and Titan. *Space. Sci. Rev.*, 106, 121-138.
- Paardekooper, S.-J., and Mellema, G. (2006) Dust flow in gas disks in the presence of embedded planets. *Astron. Astrophys.*, 453, 1129-1140.
- Podolak, M., Pollack, J. B., and Reynolds, R. T. (1988) Interactions of planetesimals with proto-planetary atmospheres. *Icarus*, 73, 163-179.
- Pollack, J. B., and Reynolds, R. T. (1974) Implications of Jupiter's early contraction history for the composition of the Galilean satellites. *Icarus*, 21, 248-253.
- Pollack, J. B., Grossman, A. S., Moore, R., and Graboske Jr., H. C. (1976) The formation of Saturn's satellites and rings as influenced by Saturn's contraction history. *Icarus*, 29, 35-48.
- Pollack, J. B., Grossman, A. S., Moore, R., and Graboske Jr., H. C. (1977) A calculation of Saturn's gravitational contraction history. *Icarus*, 30, 111-128.
- Pollack, J. B., Hollenbach, D., Beckwith, S., Simonelli, D. P., Roush, T., and Fong, W. (1994) Composition and radiative properties of grains in molecular clouds and accretion disks. *Astrophys. J.*, 421, 615-639.
- Pollack, J. B., Hubickyj, O., Bodenheimer, P., Lissauer, J. J., Podolak, M., and Greenszeg, Y. (1996) Formation of the giant planets by concurrent accretion of solids and gas. *Icarus*, 124, 62-85.
- Porco, C. C., and 34 colleagues (2005) Cassini imaging science: Initial results on Saturn's rings and small satellites. *Science*, 307, 1226-1236.
- Prialnik, D., and Podolak, M. (1995) Radioactive heating of porous comet nuclei. *Icarus*, 117, 420-430.
- Quillen, A. C., and Trilling, D. E. (1998) Do proto-jovian planets drive outflows? *Astrophys. J.*, 508, 707-713.
- Rafikov, R. R. (2002a) Nonlinear propagation of planet-generated tidal waves. *Astrophys. J.*, 569, 997-1008.
- Rafikov, R. R. (2002b) Planet migration and gap formation by tidally induced shocks. *Astrophys. J.*, 572, 566-579.
- Rafikov, R. R. (2005) Can Giant Planets Form By Direct Gravitational Instability? *Astrophys. J.*, 621, L69-L69.
- Rice, W. K. M., Armitage, P. J., Wood, K., and Lodato, G. (2006) Dust filtration at gap edges: implications for the spectral energy distributions of discs with embedded planets. *Mon. Not. Roy. Astron. Soc.*, 379, 1619-1626.
- Ruskol, E. L. (1975) In *Origin of the Moon*. NASA Transl. into English of the book "Proiskhozhdeniye Luna", pp. 1-188. Nauka Press, Moscow.
- Ruskol, E. L. (1981) Formation of planets. In *The Solar System and Its Exploration*, ESA, pp. 107-113 (SEE N82-26087 16-88).
- Ruskol, E. L. (1982) Origin of planetary satellites. *Izv. Earth Phys.*, 18, 425-433.

- Ryu, D., and Goodman, J. (1992) Convective instability in differentially rotating disks. *Astrophys. J.*, 308, 438-450.
- Safronov, V. S. (1960) On the gravitational instability in flattened systems with axial symmetry and non-uniform rotation. *Annales d'Astrophysique*, 23, 979-982.
- Safronov, V. S. (1969) Evolution of the protoplanetary cloud and formation of the Earth and planets. Nauka, Moscow. [Transl.: Israel Program for Scientific Translations, 1972. NASA TTF-667].
- Safronov, V. S., and Ruskol, E. L. (1977) The accumulation of satellites. In *Planetary Satellites*, (J. A. Burns, ed.), pp. 501-512. University of Arizona Press, Tucson.
- Safronov, V. S., Pechernikova, G. V., Ruskol, E. L., and Vitiazev, A. V. (1986) Protosatellite swarms. In *Satellites*, (J. A. Burns, and M. S. Matthews, eds.), pp. 89-116, University of Arizona Press, Tucson.
- Sandford, S. A., and 54 colleagues (2006) Organics captured from comet 81P/Wild 2 by the Stardust spacecraft. *Science*, 314, 1720-1725.
- Sari, R., and Goldreich, P. (2004) Planet-Disk Symbiosis. *Astrophys. J.*, 606, L77-L80.
- Sari, R., and Goldreich, P. (2006) Spherical accretion. *Astrophys. J.*, 642, L65-L67.
- Sasselov, D. D., and Lecar, M. (2000) On the snow line in dusty protoplanetary disks. *Astrophys. J.*, 528, 995-998.
- Schlichting, H. E., and Sari, R. (2007) Formation of Kuiper belt binaries. *Astrophys. J.*, in press.
- Schmidt, O. Yu. (1957) Four lectures on the theory of the origin of the Earth. Third ed., NA SSSR Press, Moscow.
- Schmitt, B., Espinasse, S., Grim, R. J. A., Greenberg, J. M., and Klinger, J. (1989) Laboratory studies of cometary ice analogues. In *ESA, Physics and Mechanics of Cometary Materials*, pp. 65-69.
- Schubert, G., Anderson, J. D., Spohn, T., and McKinnon, W. B. (2004) Interior composition, structure and dynamics of the Galilean satellites. In *Jupiter. The planet, satellites and magnetosphere*, (F. Bagenal, T. E. Dowling, and W. B. McKinnon, eds.), pp. 281-306. Cambridge planetary science, Vol. 1, Cambridge, UK: Cambridge University Press.
- Scott, E. R. D., and Krot, A. N. (2005) Thermal processing of silicate dust in the solar nebula: Clues from primitive chondrite matrices. *Astrophys. J.*, 623, 571-578.
- Sekiya, M. (1998) Quasi-equilibrium density distributions of small dust aggregations in the Solar Nebula. *Icarus*, 133, 298-309.
- Shakura, N. I., and Sunyaev, R. A. (1973) Black holes in binary systems. Observational appearance. *Astron. Astrophys.*, 24, 337-355.
- Shen, Y., Stone, J. M., and Gardiner, T. A. (2006) Three-dimensional Compressible Hydrodynamic Simulations of Vortices in Disks. *Astrophys. J.*, 653, 513-524.
- Shoemaker, E. M. (1984) Kuiper Prize Lecture, 16th DPS meeting, Kona, HI.
- Showalter, M. R. (1991) Visual detection of 1981S13, Saturn's eighteenth satellite, and its role in the Encke gap. *Nature*, 351, 709-713.
- Showman, A. P., and Malhotra, R. (1997) Tidal evolution into the Laplace resonance and the resurfacing of Ganymede. *Icarus*, 127, 93-111.
- Shu, F. H., Johnstone, D., and Hollenbach, D. (1993) Photoevaporation of the solar nebula and the formation of the giant planets. *Icarus*, 106, 92-101.
- Shu, F. H., Shang, H., Gounelle, M., Glassgold, A. E., and Lee, T. (2001) The Origin of Chondrules and Refractory Inclusions in Chondritic Meteorites. *Astrophys. J.*, 548, 1029-1050.
- Sohl, F., Spohn, T., Breuer, D., and Nagel, K. (2002) Implications from Galileo Observations on the Interior Structure and Chemistry of the Galilean Satellites. *Icarus*, 157, 104-119.

- Spohn, T., and Schubert, G. (2003) Oceans in the icy Galilean satellites of Jupiter? *Icarus*, 161, 456-467.
- Stepinski, T. F., and Valageas, P. (1997) Global evolution of solid matter in turbulent protoplanetary disks. II. Development of icy planetesimals. *Astron. Astrophys.*, 319, 1007-1019.
- Stern, S. A., and Weissman, P. R. (2001) Rapid collisional evolution of comets during the formation of the Oort cloud. *Nature*, 409, 589-591.
- Stern, S. A. (2003) The evolution of comets in the Oort cloud and Kuiper belt. *Nature*, 424, 639-642.
- Stevenson, D. J. (1982) Formation of the giant planets. *Plan. Space Sci.*, 30, 755-764.
- Stevenson, D. J., Harris, A. W., and Lunine, J. I. (1986) Origins of satellites. In *Satellites*, (J. A. Burns, and M. S. Matthews, eds.), University of Arizona Press, Tucson.
- Stevenson, D. J., and Lunine, J. I. (1988) Rapid formation of Jupiter by diffuse redistribution of water vapor in the solar nebula. *Icarus*, 75, 146-155.
- Stevenson, D. J., McKinnon, W. B., Canup, R., Schubert, G., and Zuber, M. (2003) The power of JIMO for determining Galilean satellite internal structure and origin (abstract). American Geophysical Union, Fall Meeting 2003, abstract #P11C-05.
- Stewart, G. R. and Wetherill, G. W. (1988) Evolution of planetesimal velocities. *Icarus*, 74, 542-553.
- Takata, T., and Stevenson, D. J. (1996) Despin mechanism for protogiant planets and ionization state of protogiant planetary disks. *Icarus*, 123, 404-421.
- Takeuchi, T., and Lin, D. N. C. (2002) Radial Flow of Dust Particles in Accretion Disks. *Astrophys. J.*, 581, 1344-1355.
- Tanigawa, T., and Watanabe, S. (2002) Gas accretion flows onto giant protoplanets: High-resolution two-dimensional simulations. *Astrophys. J.*, 580, 506-518.
- Tsiganis, K., Gomes, R., Morbidelli, A., and Levison, H. F. (2005) Origin of the orbital architecture of the giant planets of the Solar System. *Nature*, 435, 459-461.
- Turner, N. J., Sano, T., and Dziourkevitch, N. (2007) Turbulent mixing and the dead zone in protostellar disks. *Astrophys. J.*, 659, 729-737.
- Umurhan, O. M., and Regev, O. (2004) Hydrodynamic stability of rotationally supported flows: Linear and nonlinear 2D shearing box results. *Astron. Astrophys.*, 427, 855-872.
- Völk, H. J., Morfill, G. E., Roeser, S., and Jones, F. C. (1980) Collisions between grains in a turbulent gas. *Astron. Astrophys.*, 85, 316-325.
- Wadhwa, M., Amelin, Y., Davis, A. M., Lugmair, G. W., Meyer, B., Gounelle, M., and Desch, S. J. (2007) From dust to planetesimals: Implications for the Solar protoplanetary disk from short-lived radionuclides. In *Protostars and Planets V*. (B. Reipurth, D. Jewitt, and K. Keil, eds.), pp. 835-848. University of Arizona Press, Tucson.
- Ward, W. R. (1997) Protoplanet migration by nebula tides. *Icarus*, 126, 261-281.
- Weidenschilling, S. J. (1977a) Aerodynamics of solid bodies in the solar nebula. *Mon. Not. Roy. Astron. Soc.*, 180, 57-70.
- Weidenschilling, S. J. (1977b) The distribution of mass in the planetary system and solar nebula. *Astrophys. Space Sci.*, 51, 153-158.
- Weidenschilling, S. J. (1984) Evolution of grains in a turbulent solar nebula. *Icarus*, 60, 553-567.
- Weidenschilling, S. J. (1988) Formation processes and timescales for meteorite parent bodies. In *Meteorites and the Early Solar System*, (J. F. Kerridge, M. S. Matthews, eds.), University of Arizona Press, Tucson.
- Weidenschilling, S. J. (1997) The origin of comets in the solar nebula: a unified model. *Icarus*, 127, 290-306.
- Weidenschilling, S. J. (2002) Structure of a particle layer in the midplane of the Solar Nebula: Constraints on mechanisms for chondrule formation. *Meteor. Plan. Sci.*, 37, Supp., A148

- Weidenschilling, S. J. (2004) From icy grains to comets. In *Comets II*, (M. C. Festou, H. U. Keller, and H. A. Weaver, eds.), pp. 97-104, University of Arizona Press, Tucson.
- Weidenschilling, S. J., and Davis, D. R. (1985) Orbital resonances in the solar nebula - Implications for planetary accretion. *Icarus*, 62, 16-29.
- Weidenschilling, S. J., and Cuzzi, J. N. (1993) Formation of planetesimals in the solar nebula. In *Protostars and Planets III*, (E. H. Levy and J. I. Lunine, eds.), pp. 1031-1060. University of Arizona Press, Tucson.
- Wetherill, G. W. (1980) Formation of the terrestrial planets. *Ann. Rev. Astron. Astrophys.*, 18, 77-113.
- Wetherill, G. W. (1986) Accumulation of the terrestrial planets and implications concerning lunar origin. In *Origin of the Moon*, Lunar and Planetary Institute, Houston, pp. 519-550.
- Wetherill, G. W. (1990) Formation of the Earth. *Ann. Rev. Earth Planet. Sci.*, 18, 205-256.
- Wetherill, G. W. and Stewart, G. R. (1989) Accumulation of a swarm of small planetesimals. *Icarus*, 77, 330-357.
- Wetherill, G. W. and Stewart, G. R. (1993) Formation of planetary embryos - Effects of fragmentation, low relative velocity, and independent variation of eccentricity and inclination. *Icarus*, 106, 190.
- Wilner, D. J., Ho, P. T. P., Kastner, J. H., and Rodríguez, L. F. (2000) VLA imaging of the disk surrounding the nearby young star TW Hydrae. *Astrophys. J.*, 534, L101-L104.
- Wuchterl, G., Guillot, T., and Lissauer, J. J. (2000) Giant planet formation. In *Protostars and Planets IV* (V. Mannings, A. Boss, and S. Russel, eds.), pp. 1081-1109. University of Arizona Press, Tucson.
- Wurm, G., and Blum, J. (1998) Experiments on Preplanetary Dust Aggregation. *Icarus*, 132, 125-136.
- Youdin, A. N., and Shu, F. H. (2002) Planetesimal formation by gravitational instability. *Astrophys. J.*, 580, 494-505.
- Youdin, A. N., and Chiang, E. I. (2004) Particle pileups and planetesimal formation. *Astrophys. J.*, 601, 1109-1119.
- Young, R. E. (2003) The Galileo probe: how it has changed our understanding of Jupiter. *New Astron. Revs.*, 47, 1-51.
- Yurimoto, H., Kuramoto, K., Krot, A. N., Scott, E. R. D., Cuzzi, J. N., Thieme, M. H., and Lyons, J. R. (2007) Origin and evolution of oxygen-isotopic compositions in the solar system. In *Protostars and Planets V*, (B. Reipurth, D. Jewitt, and K. Keil, eds.), pp. 849-862. University of Arizona Press, Tucson.
- Zimmer, C., Khurana, K. K., and Kivelson, M. G. (2000) Subsurface oceans on Europa and Callisto: Constraints from Galileo magnetometer observations. *Icarus*, 147, 329-347.
- Zolensky, M. E., and 74 colleagues (2006) Minerology and petrology of comet 81P/Wild 2 nucleus samples. *Science*, 314, 1735-1741.